Atmos. Chem. Phys. Discuss., 12, 14269–14327, 2012
www.atmos-chem-phys-discuss.net/12/14269/2012/
doi:10.5194/acpd-12-14269-2012

Atmospheric Chemistry and Physics Discussions

Model uncertainties affecting satellite-based inverse modeling of nitrogen oxides emissions and implications for surface ozone simulation

J.-T. Lin[1], Z. Liu[2], Q. Zhang[3], H. Liu[4], J. Mao[5,6], and G. Zhuang[7]

[1]Laboratory for Climate and Ocean-Atmosphere Studies, Department of Atmospheric and Oceanic Sciences, School of Physics, Peking University, Beijing 100871, China
[2]School of Earth and Atmospheric Sciences, Georgia Institute of Technology, Atlanta, Georgia 30332, USA
[3]Center for Earth System Science, Tsinghua University, Beijing, China
[4]National Institute of Aerospace, Hampton, VA 23666, USA
[5]Program in Atmospheric and Oceanic Sciences, Princeton University, Princeton, NJ 08542, USA
[6]Geophysical Fluid Dynamics Laboratory/National Oceanic and Atmospheric Administration, Princeton, NJ 08542, USA
[7]Center for Atmospheric Chemistry Study, Department of Environmental Science and Engineering, Fudan University, Shanghai, 200433, China

Received: 22 April 2012 – Accepted: 29 May 2012 – Published: 7 June 2012

Correspondence to: J.-T. Lin (linjt@pku.edu.cn)

Published by Copernicus Publications on behalf of the European Geosciences Union.

Abstract

Errors in chemical transport models (CTMs) interpreting the relation between space-retrieved tropospheric column densities of nitrogen dioxide (NO_2) and emissions of nitrogen oxides (NO_x) have important consequences on the inverse modeling. They are however difficult to quantify due to lack of adequate in situ measurements, particularly over China and other developing countries. This study proposes an alternate approach for model evaluation over East China, by analyzing the sensitivity of modeled NO_2 columns to errors in meteorological and chemical parameters/processes important to the nitrogen abundance. As a demonstration, it evaluates the nested version of GEOS-Chem driven by the GEOS-5 meteorology and the INTEX-B anthropogenic emissions and used with retrievals from the Ozone Monitoring Instrument (OMI) to constrain emissions of NO_x. The CTM has been used extensively for such applications. Errors are examined for a comprehensive set of meteorological and chemical parameters using measurements and/or uncertainty analysis based on current knowledge. Results are exploited then for sensitivity simulations perturbing the respective parameters, as the basis of the following post-model linearized and localized first-order modification. It is found that the model meteorology likely contains errors of various magnitudes in cloud optical depth, air temperature, water vapor, boundary layer height and many other parameters. Model errors also exist in gaseous and heterogeneous reactions, aerosol optical properties and emissions of non-nitrogen species affecting the nitrogen chemistry. Modifications accounting for quantified errors in 10 selected parameters increase the NO_2 columns in most areas with an average positive impact of 22 % in July and 10 % in January. This suggests a possible systematic model bias such that the top-down emissions will be overestimated by the same magnitudes if the model is used for emission inversion without corrections. The modifications however cannot account for the large model underestimates in cities and other extremely polluted areas (particularly in the north) as compared to satellite retrievals, likely pointing to underestimates of the a priori emission inventory in these places with important implications for understanding of atmospheric chemistry and air quality. Post-model modifications also have large impacts on surface ozone concentrations with the peak values in July over North China decreasing by about 15 ppb. Individually, modification for the uptake of the hydroperoxyl radical on aerosols has the largest impact for both NO_2 and ozone, followed by various other parameters important for some species in some seasons. Note that these modifications are simplified and should be used with caution for error apportionment.

1 Introduction

Anthropogenic emissions of nitrogen oxides ($NO_x \equiv NO + NO_2$) in China have been growing at an average rate of about 8 % per year (Richter et al., 2005; Zhang et al., 2007; Lamsal et al., 2011; Lin and McElroy, 2011) over the past decade, disrupted temporarily by various socioeconomic events such as the economic downturn, Olympics and Chinese New Year (Mijling et al., 2009; Lin et al., 2010a; Lin and McElroy, 2011). The rising emissions have attracted tremendous attention concerning the consequences on tropospheric chemistry, air pollution, climate forcing and acid deposition over both source and downwind regions (e.g., Streets et al., 2003; Richter et al., 2005; Martin et al., 2006; Zhang et al., 2007; Stavrakou et al., 2008; Lin et al., 2010a; Lin, 2012).

Simulations of chemical transport models (CTMs) are employed extensively with space based measurements of vertical column densities of tropospheric nitrogen dioxide (NO_2) to constrain emissions and variability of NO_x in China from the top-down perspective (e.g., Jaeglé et al., 2005; van der A et al., 2006; Lin and McElroy, 2011; Lin, 2012). Such top-down constraint is a useful supplement to bottom-up estimates which are subject to uncertainties in emission factors and emission activities (Streets et al., 2003; Zhang et al., 2007, 2009b). It is however affected by errors not just in satellite retrievals but also in CTMs simulating the fate of nitrogen emitted into the troposphere (Martin et al., 2006; Zhao and Wang, 2009; Lin et al., 2010b; Lin, 2012).

Errors in model simulations are estimated often from ground-based and aircraft measurements of nitrogen, mostly in a short time period, over the developed countries or over remote/downwind regions (e.g., Hudman et al., 2007; Brinksma et al., 2008; Boersma et al., 2009; Lamsal et al., 2010; Lin and McElroy, 2010). Conclusions drawn are adopted for China and other countries/regions where in situ measurements are not available (Jaeglé et al., 2005; Martin et al., 2006; Boersma et al., 2008; Zhao and Wang, 2009; Lin et al., 2010b; Wang et al., 2012). However, the magnitude and causes of model errors may be region and time dependent, resulting in uncertainties in the applicability of findings from model evaluation limited in time and space. For example, errors in model meteorology may depend on locations and seasons; and errors in heterogeneous reactions on aerosol surfaces are important mainly at locations with high aerosol loadings (see Sects. 4 and 5). Even for areas with nitrogen observations, it is still difficult to evaluate the model capability in relating emissions and atmospheric abundances based on measured concentrations alone without accurate information on emissions. Lin and McElroy (2010) evaluated the modeled vertical mixing in the planetary boundary layer (PBL) over the Northeast USA using aircraft observations. They noted that modeled concentrations of NO_2 are much lower than observed values throughout the PBL, which may or may not be caused entirely by emission errors.

The present study proposes an alternate approach for model evaluation over China, by analyzing the sensitivity of simulated NO_2 columns to model meteorological and chemical parameters of importance to the nitrogen chemistry (Fig. 1). A large number of sensitivity simulations are conducted to evaluate the impacts of errors in model meteorological fields constrained by ground and space based measurements. The model chemistry is evaluated with additional simulations addressing the embedded errors/uncertainties based on current understanding. Improvements on the estimate of NO_2 columns are achieved then by linearized and localized first-order modifications accounting for quantified errors in model meteorological and chemical parameters. The method is useful for China due particularly to lack of adequate and timely measurements of nitrogen constituents for more direct model evaluation.

As a demonstration, this study evaluates tropospheric NO_2 columns simulated by the nested GEOS-Chem model (Chen et al., 2009) in use of inferring emissions of NO_x from NO_2 columns retrieved from the Ozone Monitoring Instrument (OMI). GEOS-Chem has been used extensively for such top-down constraints over a variety of temporal and spatial scales (Jaeglé et al., 2005; Martin et al., 2006; Boersma et al., 2008; Zhang et al., 2008; Lin et al., 2010b; Lamsal et al., 2011; Lin and McElroy, 2011; Lin, 2012; Wang et al., 2012). Findings from the analysis of GEOS-chem simulations may be applicable to some extent to other models with different meteorological data and/or chemical schemes. The analysis is focused in East China (101.25°–126.25° E, 19°–46° N) concerning the extensive inverse modeling studies addressing its significant and rapidly increasing emissions of NO_x in recent years (e.g., Richter et al., 2005; Zhang et al., 2007; Stavrakou et al., 2008; Lin, 2012). Simulations for January and July 2006 are both evaluated to account for potential seasonal dependence of model errors.

Errors in model meteorological and chemical parameters also have significant implications for other model applications. The impacts on surface ozone simulation are analyzed in the present study to further demonstrate the importance of explicitly accounting for model errors in respective applications.

The remaining sections are organized as follows. Section 2 presents meteorological observations from the ground networks and satellite remote sensing, as well as space based measurements of aerosol optical depth (AOD) and NO_2 columns. Section 3 presents the CTM simulations and a brief comparison with satellite retrievals. Sections 4 and 5 evaluate the impacts on simulated NO_2 columns of potential errors in model meteorological and chemical parameters, respectively, by employing a large set of sensitivity simulations. The test simulations are conducted based current understanding of the nitrogen chemistry, as shown in Fig. 1. Section 6 makes an attempt to modify the simulated NO_2 columns on the first order accounting for quantified errors in model meteorology and chemistry. Implications of potential meteorological and chemical errors for simulations of surface ozone are discussed in Sect. 7. Section 8 summarizes the present study.

2 Ground and space measurements

2.1 Meteorological observations

Ground measurements for January and July 2006 are taken from the National Oceanic and Atmospheric Administration (NOAA) National Climatic Data Center (NCDC) Integrated Surface Hourly (ISH) dataset (DS3505) for a variety of meteorological parameters, including air temperature, relative humidity (RH), surface air pressure, wind speed at 10 m, and precipitation. The ISH dataset combines measurements from various networks publically available for weather and climate analyses. It was used by Lin and McElroy (2011) to analyze the day-to-day variation of meteorology in January 2009 of relevance to changes in NO_2 columns retrieved from space and simulated by GEOS-Chem. Here meteorological data are taken from a total of 284 stations across East China. They are available every three hours (starting from 00:00 UTC) with the exception of daily precipitation data.

Space measurements of tropospheric water vapor path, cloud fraction and cloud optical depth (COD) are taken from the International Satellite Cloud Climatology Project (ISCCP) D2 dataset. The ISCCP dataset is used widely in studies of clouds and the hydrological cycle. It provides monthly mean data on the 2.5° long × 2.5° lat grid for time of day from 00:00 to 21:00 UTC at 3-h intervals for cloud fraction and COD, and monthly mean daily mean data for water vapor path. Here data for January and July 2006 are sampled at the locations of ground meteorological stations for comparison with the GEOS-5 meteorology.

2.2 NO_2 columns from OMI

Retrievals of NO_2 columns are taken from the DOMINO product version 2 (Boersma et al., 2011). The processing of DOMINO-2 is presented in Lin (2012), including but not limited to the conversion from level 2 to level 3 monthly data and an analysis of retrieval errors. The level 3 data are derived on the 0.25° long × 0.25° lat grid for January and July 2006.

2.3 MODIS AOD

To evaluate modeled optical properties of aerosols, measurements of aerosol optical depth (AOD) at 550 nm are taken from the MODIS/Aqua level 2 collection 5.1 product. Data for January and July 2006 are sampled at the locations of ground meteorological stations for comparison with GEOS-Chem simulations. For a given station, valid MODIS data in each day available within 0.25° of the station are averaged to obtain the daily value.

3 GEOS-Chem simulation and comparison with OMI retrievals

This study evaluates the nested model for Asia (Chen et al., 2009) of GEOS-Chem (version 8-03-02; http://wiki.seas.harvard.edu/geos-chem/index.php/MainPage). The model is driven by the assimilated meteorological fields of GEOS-5 taken from the National Aeronautics and Space Administration (NASA) Global Modeling and Assimilation Office (GMAO). It is run with the full O_x-NO_x-CO-VOC-HO_x chemistry and online calculation for various aerosols (sulfate, nitrate, ammonium, black carbon, primary organic carbon, sea salt and dust). The nested model has a horizontal resolution of 0.667° long × 0.5° lat with 47 vertical layers; and each of the lowest 10 layers is about 130 m thick. Its lateral boundary conditions are updated every 3 h from a respective global simulation at 5° long × 4° lat. Other model setup is described in more detail in Lin (2012), including emissions and their temporal variability. In particular, anthropogenic emissions in Asia are taken from the INTEX-B inventory as representative of 2006 (Zhang et al., 2009b) for various species including NO_x, carbon monoxide (CO), non-methane volatile organic compounds (VOC), sulfur dioxide (SO_2), black carbon (BC) and primary organic carbon (OC).

For all simulations (see Table 1), modeled vertical distribution of NO_2 in each day is sampled at the time with valid retrievals, regridded to 0.25° long × 0.25° lat, and applied with the averaging kernel (AK) from DOMINO-2. The daily data are averaged then to obtain monthly mean values in January and July 2006 for the present analysis.

NO_2 columns derived from the base simulation (Case 1 in Table 1) are compared in detail to retrieved values by Lin (2012). Averaged over East China, model NO_2 columns are lower than the retrievals by about 20 % in July and by 36 % in January. The underestimate is much more significant in extremely polluted areas such as cities and locations with large point sources, particularly in the north in January: model values are only about 20–30 % of retrievals. Results are similar from the comparison at the 284 meteorological stations showing a slope of about 0.5 in both months under the reduced major axis (RMA) regression (Fig. 2a, b). Lin (2012) found that total anthropogenic emissions of NO_x in East China inferred from DOMINO-2 are larger than the INTEX-B inventory by about 40 %. These differences are attributable in part to errors in model simulations, as analyzed in the following sections.

4 Sensitivity of GEOS-Chem simulations to meteorological parameters

Errors in the GEOS-5 meteorological fields have consequences on a variety of atmospheric processes affecting the abundance of tropospheric NO_2 simulated by GEOS-Chem. The GEOS-5 meteorology is evaluated in the Supplement with Figs. S1–S8 using observational data from ISH and ISCCP. Parameters analyzed include air temperature, RH, tropospheric water vapor path, air pressure, wind speed, cloud fraction, COD and precipitation. The analysis is emphasized in the daytime, particularly at midday when the lifetime of NO_x is shortest and has the largest impact on its abundance at the overpass time of OMI (i.e., in the early afternoon).

In this section, sensitivity simulations are conducted to evaluate the impacts of errors in air temperature, water vapor content and COD on modeled NO_2 columns, by adjusting the respective parameters in GEOS-Chem (see Fig. 1 and Table 1). Also analyzed are the impacts of potential errors in convection (and resulting lightning emissions of NO_x) and vertical mixing in the PBL.

Errors in RH affect wet deposition of various species and hygroscopic growth of aerosols. These factors are accounted for implicitly with adjusted air temperature and water vapor as the CTM re-calculates RH on the fly. Impacts of errors in 10 m wind speed on modeled NO_2 columns are mainly on the local scale due to the relatively short lifetime of NO_x. Also, biases in wind speed are likely limited to altitudes close to the ground where small-scale variability is not captured by GEOS-5, as expected for an assimilation product (Pryor and Barthelmie, 2011). At higher altitudes, wind speed is better constrained, since the large-scale circulation is reasonably reproduced by GEOS-5 (as suggested by the evaluation for surface air pressure in the Supplement). Errors in precipitation are small averaged over East China (see Supplement). They are also not very important for the simulation of NO_x whose wet scavenging is relatively weak. Therefore the impacts of these parameters on modeled NO_2 columns are not evaluated explicitly in the present study.

4.1 Air temperature

Errors in air temperature affect the calculation of gaseous and heterogeneous reactions, deposition and biogenic emissions of volatile organic compounds (VOC), with consequences on modeled NO_2 columns. Their overall impact is evaluated here by sensitivity simulations perturbing air temperature in GEOS-5 (Cases 2–5 in Table 1), based on analysis of temperature in the Supplement.

The first simulation increases the nighttime temperature by 1 °C and decreases the daytime temperature by 2 °C in the lowest 10 model layers (about 0–1.3 km above the ground) (Case 2 in Table 1). The adjustment extends to the lower troposphere to account for potential errors that may be transported from near the ground to the entire PBL. It also affects the ground temperature with consequences on modeled biogenic emissions. As a result, modeled NO_2 columns in July are reduced by 0–4 % over most regions with enhancements by up to 10 % in parts of the southwest (Fig. S9a). This is mainly a result of enhanced formation of nitric acid (through enhanced $NO_2 + OH$ reaction, a termolecular reaction with negative dependence on temperature) compensated by reduced production of organic nitrates (through reduced emissions of VOC). For January, model NO_2 columns are reduced by up to 8 % in some areas (Fig. S9b).

The daytime biases in air temperature exceed 5 °C in parts of East China (Fig. S1). Therefore another sensitivity simulation as an extreme case increases the daytime temperature by 5 °C with a reduction by 1 °C at night (Case 3 in Table 1). It reduces model NO_2 columns by 4–10 % in many areas of East China for both months (Fig. 3). In part of the southwest, model NO_2 columns are enhanced by up to 16 % in July. Assuming a weaker effect of PBL mixing on temperature errors, the temperature adjustment is constrained to the lowest four model layers (i.e., about 0–500 m above the ground) in a further simulation (Case 4 in Table 1). This tends to slightly increase the NO_2 columns relative to when the temperature is adjusted for the lowest 10 layers (Fig. S9e, f versus Fig. 3).

The nighttime temperature errors are not important for simulation of NO_2 columns in the afternoon. This is suggested by an additional simulation increasing the nighttime temperature by 5 °C with no changes in the daytime (Case 5 in Table 1). Specifically, the sensitivity test results in insignificant changes in model NO_2 columns in both months: within 2 % for July and within 4 % in most areas for January (not shown).

4.2 Water vapor content

Water vapor content in the troposphere affects the yield of hydroxyl radical (OH) from ozone photolysis and consequently the loss rate of NO_x via OH oxidation. It also affects the hygroscopic growth of hydrophilic aerosols and resulting scattering efficiency for solar radiation. Based on analysis of the GEOS-5 water vapor path in the Supplement, two test simulations are conducted to quantify the sensitivity of model NO_2 columns to errors in water vapor content in GEOS-5. In particular, the water vapor content is scaled up and down, respectively, by a factor of 130 % in all tropospheric layers (Cases 6–7 in Table 1). Increasing the water vapor content results in 4–10 % reductions in

NO_2 columns across East China in July with a smaller impact for January (Fig. 4a, b). Decreasing the water vapor content has opposite impacts on model NO_2 columns for both months (Fig. 4c, d).

4.3 Cloud optical depth

Model errors in COD affect the calculation of photolysis for a variety of gaseous tracers (Liu et al., 2009). The COD in GEOS-5 is lower than 50 % of the ISCCP values in most areas of East China for both January and July (Fig. S7). Here four sensitivity simulations are performed to evaluate the effect of COD on model photolysis and resulting NO_2 columns, by multiplying the COD by a factor of 0 %, 50 %, 150 % and 200 %, respectively (Cases 8–11 in Table 1). The resulting impacts on NO_2 columns are significant especially in the eastern and southern provinces in July (Figs. 5, S10a–h). In particular, doubling the COD in July enhances modeled NO_2 columns by 20 % or more in many places (Fig. 5), by decreasing solar radiation in the lower troposphere allowed for photodissociation of ozone and NO_2 and formation of OH.

At a given COD, the altitude of clouds affects the vertical distribution of radiation and photolytic activities. In lack of measurements of cloud vertical distribution, the effect of potential model errors is evaluated by a sensitivity simulation distributing the COD evenly in all vertical layers within the troposphere (Case 12 in Table 1). For July, most clouds in GEOS-5 are located in the upper troposphere (not shown), thus the arbitrary change in cloud vertical profile allows more solar radiation to reach the lower troposphere. This results in a significant increase in the tropospheric OH content with a reduction in NO_2 by up to 16 % (Fig. S10i). For January, most clouds are located in the lower troposphere, especially in the south (not shown); thus the arbitrarily assumed distribution of COD results in slight increases of NO_2 over these regions (Fig. S10j).

4.4 Planetary boundary layer height (PBLH)

Vertical mixing in the PBL of nitrogen and other species affect the non-linear chemical processes in the lower troposphere. Accurate simulation of vertical mixing is important particularly for comparison with satellite retrievals when the altitude-dependent AK (i.e., satellite sensitivity to changes in NO_2 concentrations) is applied to modeled vertical distribution of NO_2. In lack of direct observations to evaluate the simulation of PBL mixing for East China, the impact of potential errors is analyzed here by adjusting the PBLH, a key parameter constraining the vertical mixing, in GEOS-Chem (Cases 13–18 in Table 1). In addition to the impacts on the nonlinear chemistry, increasing the PBLH results in enhanced vertical mixing which lifts NO_2 to higher altitudes with larger AK and thus enhances the NO_2 column (proxy); and decreasing the PBLH has an opposite effect.

The current GEOS-Chem employs a non-local scheme (Holtslag and Boville, 1993) to determine the extent of vertical mixing in the PBL, with the PBLH taken directly from GEOS-5 (Lin and McElroy, 2010). The GEOS-5 PBLH is diagnosed as the height of the lowest layer in which the eddy diffusivity is smaller than $2\,m^2\,s^{-1}$ (Global Modeling and Assimilation Office, 2006). Across East China, its values in the afternoon (13:00–15:00 Beijing local time; around the overpass time of OMI) exhibit significant seasonal variation due to changes in static and mechanic instability. In July, the afternoon height exceeds 2000 m over the arid/semiarid northwest but is only about 1000 m in the coastal provinces in the east and south (Fig. S11). In January, it reaches 2000 m in parts of Sichuan but is as low as about 750 m in the north (Fig. S11). At night, the PBLH in GEOS-5 is less than 100 m in most days of the two months over China and other continental areas (not shown). Overall, the GEOS-5 PBLH may be overestimated in the daytime due to positive biases in surface air temperature enhancing the static instability; while it may be underestimated at night as a result of negative temperature biases. The observation-based analysis for the USA by Liu and Liang (2010) suggested the nighttime PBLH to be about 200–300 m in all seasons, about 3 times as large as the GEOS-5 values.

To evaluate the importance of PBLH for modeled NO_2 columns, a sensitivity simulation calculates the height on the fly using the non-local scheme (Case 13 in Table 1). For July, this increases the afternoon PBLH over the southeast and northwest with reductions over the southwest (Fig. S11). Consequently, model NO_2 columns are enhanced by 0–4 % near the northern boundary of China, but are reduced by 0–4 % in most areas (Fig. 6a). For January, the derived PBLH in the afternoon is higher than the GOES-5 values by 100–200 m over North China but is lower over the vast west (Fig. S11). As a result, model NO_2 columns decrease by 2–12 % over most of East China with enhancements by up to 8 % in several provinces (Fig. 6b).

A second sensitivity simulation is conducted by decreasing the PBLH by 10 % in the daytime and tripling the height at night to account for their potential biases (Case 14 in Table 1). For July, this enhances model NO_2 columns by 0–6 % over most regions (Fig. 6c). For January, changes in model NO_2 columns are more inhomogeneous spatially (Fig. 6d). The effects are driven mainly by the enhanced nighttime PBLH, since the adjustment is relatively small for the daytime PBLH. This is confirmed by another simulation tripling the nighttime PBLH with no adjustment in the daytime (Case 15 in Table 1; figures are not shown).

To further test the model sensitivity to PBLH, an additional simulation employs the height data from the GEOS-4 meteorological fields to adjust values in GEOS-5 (Case 16 in Table 1). For a given location and time of day, the ratio of monthly mean GEOS-4 over GEOS-5 PBLH available on the 2.5° long × 2° lat grid is used to scale the high-resolution GEOS-5 data. The GEOS-4 PBLH is in general higher than GEOS-5 in the nighttime with closer agreement to the observation-based estimate by Liu and Liang (2010). For the mid-day PBLH, the GEOS-4 data are lower than GEOS-5 over most of East China in January (Fig. S12), resulting in reductions of model NO_2 columns by 0–20 % in many areas (Fig. 6f). They however exceed the GEOS-5 values in the northeast with a consequent increase in model NO_2 columns. In July, the impacts of PBLH adjustments are within 4 % in most areas for model NO_2 columns (Fig. 6e).

Since NO_2 columns from the base simulation are lower than satellite retrievals by about 20 % in July and 36 % in January averaged over East China, we further test the possibility that the differences originate from errors in modeled PBL mixing. As such, the PBLH is scaled up by 130 % and 200 %, respectively, in two sensitivity simulations (Cases 17–18 in Table 1). For July, increasing the PBLH by 30 % enhances the NO_2 columns by 0–10 % over most regions (Fig. S13a). The 100 % increase in PBLH results in enhancements of model NO_2 columns by 10–20 % over a large portion of East China (Fig. 14c). The impacts in January are much larger than that for July: model NO_2 columns are enhanced by 10–20 % (20–50 %) in many areas of the east and south when the PBLH is enhanced by 30 % (100 %) (Fig. S13b, d).

4.5 Convection and consequent lightning emissions

Convection affects the vertical distributions of NO_x and other species by transporting pollutants between the lower and upper troposphere. It however is highly parameterized and subject to large uncertainties in current models (Tost et al., 2010). As indicators of convection, the cloud amount is underestimated by GEOS-5 while precipitation is reproduced relatively well on the regional mean basis (see Supplement Sects. S1.6 and S1.7). Therefore it is currently unclear about the magnitude of convection errors in GEOS-5 and consequent impacts on simulations of GEOS-Chem. Lin (2012) conducted a sensitivity analysis assuming a 50 % increase in the convection of NO_2 of anthropogenic origin. They consequently found an increase by 7.5 % in anthropogenic NO_2 columns averaged over East China (when the averaging kernel is applied to modeled vertical distribution of NO_2). Further research is needed to improve the understanding of convection and its representation in the model.

Convection results in lightning flashes and consequent emissions of NO_x. The importance of lightning emissions is affected also by the yield of nitric oxide (NO) from each flash and its vertical distribution, which processes are not well understood (Sauvage et al., 2007). The contribution of a given amount of lightning emissions to model NO_2 columns (when the AK is implemented) is found to be about 50 % larger than that of anthropogenic emissions averaged over East China (Lin et al., 2010b; Lin, 2012). The inverse modeling by Lin (2012) suggested that GEOS-Chem underestimates lightning emissions in East China by 14 % in July 2006 and by 19 % for the entire year. The exact causes of the biases are not clear, however.

5 Sensitivity of GEOS-Chem simulations to chemical parameters

Originally developed as a global CTM, GEOS-Chem adopts a simplified chemical scheme to reduce the complexness and computational cost for global and regional analyses, as compared to more detailed schemes such as MCM 3.2 (Saunders et al., 2003). It has been suggested that the GEOS-Chem chemical scheme produces relatively consistent results with MCM 3.1 for inorganic gaseous chemistry, taking into account differences in the kinetic data used (JPL versus IUPAC) (Emmerson and Evans, 2009). The differences increase for organic gaseous chemistry (Emmerson and Evans, 2009), as expected for a largely simplified chemical scheme, with potentially important implications for the nitrogen evolution over areas with abundant VOC. In addition, the implementation of heterogeneous reactions and kinetic data differs between current chemical schemes. In particular, GEOS-Chem mainly adopts the kinetic data from the Jet Propulsion Laboratory (JPL) (Sander et al., 2011), differing from the IUPAC data (Atkinson et al., 2004, 2006) employed in MCM and some other schemes. Therefore the sensitivity analysis here is concentrated on chemical parameters/processes that have been identified to be important for the nitrogen chemistry in general (rather than specific ally to GEOS-Chem) (see Fig. 1 and Table 1). Results here can thus be applied to some extent to other (and maybe more sophisticated) chemical schemes.

5.1 Rate constant for reaction of OH and NO_2

Reaction of OH + NO_2 producing nitric acid ($HONO_2$, or HNO_3) is the primary sink of NO_x in the troposphere. Recent lab experiments suggested a second pathway producing pernitrous acid (HOONO) with a branching ratio of 5–15 % under atmospheric conditions (Sander et al., 2011). The newly found pathway has not been accounted for explicitly in the current GEOS-Chem model since HOONO is likely unstable and easily converted back to NO_2. It is excluded from the analysis hereafter.

The current GEOS-Chem adopts the rate constant for the nitric acid branch recommended by the JPL with an uncertainty of 30 % at 298 K (Sander et al., 2011). A recent lab study suggested the rate constant to be about 15 % lower than the JPL value at 298 K without specifying the values at other temperatures (Mollner et al., 2010), in support of some previous studies indicating the current JPL value to be biased high (Okumura and Sander, 2005). Here two sensitivity simulations are performed to evaluate the impact of potential errors in the rate constant on modeled NO_2 columns, by scaling up and down, respectively, the rate constant by a factor of 130 % (Cases 19–20 in Table 1). Decreasing the rate constant enhances model NO_2 columns by 10–20 % across East China in July and by 0–10 % in January (Fig. 7a, b). Increasing the rate constant has an opposite effect of similar magnitude (not shown).

5.2 Yield of HNO_3 from reaction of NO and hydroperoxyl radical (HO_2)

An important pathway of NO_2 formation is reaction of NO and HO_2. Lab experiments by Butkovskaya et al. (2005, 2007, 2009) suggested a small yield of HNO_3 during the reaction resulting in loss of NO_x. The yield depends on temperature, pressure and water vapor content. It is less than 1 % in dry air, but can be enhanced by up to an order of magnitude in the presence of water vapor (Butkovskaya et al., 2009; Sander et al., 2011). Here, two sensitivity simulations are performed by assuming a constant yield of HNO_3 at 5 % and 1 %, respectively (Cases 21–22 in Table 1). A yield of 5 % reduces model NO_2 columns by 44 % in July and by 12.5 % in January averaged over

Title Page
Abstract | Introduction
Conclusions | References
Tables | Figures
◀| |▶
◀ ▶
Back | Close
Full Screen / Esc
Printer-friendly Version
Interactive Discussion

East China with much larger impacts in many areas (Fig. 8a, b). With a yield of 1 %, model NO_2 columns are reduced by 15 % in July and by 3.4 % in January averaged over East China (Fig. 8c, d). The yield of HNO_3 and its dependence on meteorological conditions is yet to be confirmed by more lab experiments.

5.3 Isoprene chemistry and PAN

Reaction of isoprene with OH is an important process affecting the budget and partitioning of hydrogen oxide radicals (HO_x). It was assumed traditionally that the reaction resulted in conversion of OH to peroxy radicals (RO_2) and thus depletion of OH in pristine forested areas with large isoprene sources such as the Amazonian region. More recent research, however, have suggested several pathways of OH regeneration through subsequent reactions of isoprene oxidation products (Butler et al., 2008; Lelieveld et al., 2008; Kubistin et al., 2010). Here two tests are performed to evaluate the effect of isoprene oxidation and OH regeneration on model NO_2 columns. The first test assumes a 100 % regeneration of OH from the reaction of isoprene and OH (Case 23 in Table 1) (Kubistin et al., 2010, assumed 130 %). This enhances the lower tropospheric (0–2 km) OH content by up to 40 % in July over the source regions of isoprene including parts of the southern provinces and the mountain and grassland areas in the north (not shown). Consequently, model NO_2 columns decrease by 0–4 % over most regions in July with smaller changes of within 2 % in January (Fig. 9a, b). Another test is conducted by turning off the reaction of isoprene and OH to prevent the latter from being depleted (Case 24 in Table 1), following Kubistin et al. (2010). As a result, the lower tropospheric (0–2 km) OH content more than doubles in July over parts of the source regions of isoprene (not shown). Over the same regions, model NO_2 columns are increased mostly by 0–20 % with a drastic increase by 40–50 % in the southwest (Fig. 9c). The increase of NO_2 is attributed to the suppressed formation of isoprene nitrates overcompensating for the effect of enhanced HNO_3 production. The impact is smaller for January 2006 due primarily to lack of isoprene emissions (Fig. 9d).

Production of isoprene nitrates is an important sink of NO_x. It is determined by the yield of isoprene nitrates and subsequent partial conversion back to NO_x through photolysis or reactions with OH, i.e., the recycling of NO_x. In addition, certain isoprene nitrates have relatively long atmospheric lifetime and can be transported to downwind areas before being transformed to NO_x (Paulot et al., 2009). These factors affect the abundances of NO_x in source and downwind regions with important consequences on the tropospheric chemistry. For example, previous model studies have suggested large sensitivity of modeled surface ozone concentration to assumptions on production and fate of isoprene nitrates (Fiore et al., 2005; Wu et al., 2007; Lin et al., 2008a,b,c; Ito et al., 2009). The current estimates range from 2.4 % to 15 % for the net yield of isoprene nitrates (i.e., the amount that does not return to NO_x) (Chen et al., 1998; Sprengnether et al., 2002; Horowitz et al., 2003; Horowitz et al., 2007; Patchen et al., 2007; see summary by Paulot et al., 2009). A value of 10 %, on the high-end side, is adopted in GEOS-Chem by neglecting transport of the portion of isoprene nitrates decomposed to NO_x. Reducing the net yield to 2.4 %, a sensitivity simulation increases the NO_2 columns by up to 25 % over the southwest in July and by 0–6 % in January (Case 25 in Table 1; Fig. 9e, f).

Production of peroxyacetyl nitrate (PAN) balanced by its thermal decomposition also affects the abundance of NO_2. Errors in its equilibrium constant are estimated to be about 20 % at 298 K (Sander et al., 2011). A test simulation decreases the constant by 20 %, resulting in slight enhancements of model NO_2 columns by 0–4 % (within 2 % over most regions) in both January and July (Case 26 in Table 1; figures are not shown).

5.4 Heterogeneous reactions involving aerosols

Uptake of HO_2 on aerosols reduces the HO_x content in the troposphere and thus increases the NO_x lifetime. The uptake coefficient depends on aerosol types and meteorological conditions, subject to large uncertainties (Jacob, 2000; Thornton et al., 2008; Kolb et al., 2010; Mao et al., 2010; Macintyre and Evans, 2011). It can be enhanced by transition metal ions (TMIs) such as copper (Cu) and iron (Fe) contained in aqueous aerosols (Jacob, 2000; Thornton et al., 2008). Thornton et al. (2008) suggested an effective uptake coefficient of 0.04–0.1 on fine-mode pollution aerosols (radius ~ 100–200 nm) in the continental boundary layer, based on the mass fraction of Cu in near-surface aerosols observed over the contiguous USA. The average value of 0.07 is adopted in the current GEOS-Chem model for sulfate-nitrate-ammonium (SNA) aerosols with no regional dependence. The CTM does not take into account the effect of Fe, as considered to be much lower than that of Cu (Thornton et al., 2008). Meanwhile, the mass fraction of Cu measured in several cities in East China ($2.9–21.6 \times 10^{-4}$) is higher than the average value over the USA (1.8×10^{-4}) by a factor of 1.6–12 (He et al., 2001; Thornton et al., 2008; Yang et al., 2011). This is also supported by our preliminary measurement data in Beijing and Shanghai. In Beijing, the fraction of Cu doubled from 2000 to 2005 (He et al., 2001; Yang et al., 2011). Moreover, there is a large fraction of Fe in aerosols in Chinese cities (He et al., 2001; Yang et al., 2011) with potentially important impacts on the uptake of HO_2, due not just to its sole catalytic effect but also to its potential interactions with Cu enhancing the effects of both TMIs (Mao et al., 2012). Given the amount of TMIs, the uptake coefficient in these Chinese cities is likely to be much larger than currently assumed in the model. In a sensitivity simulation, the coefficient is increased to 0.2 in the troposphere over China (Case 27 in Table 1), a value consistent with previous estimates based on field measurements in North America and Hawaii (see review by Jacob, 2000). As a result, model NO_2 columns in July are enhanced by 4–14 % over North China with smaller impacts in other areas (Fig. 10a). In January, model NO_2 columns increase by up to 50 % in many areas (Fig. 10b). Another sensitivity simulation changes the uptake coefficient to 0.2 on SNA aerosols in the PBL over China (Case 28 in Table 1). It thus increases the NO_2 columns by 2–10 % over North China in July and by 2–16 % over the south in January (Fig. 10c, d).

Heterogeneous reaction of nitrogen pentoxide (N_2O_5) on aerosol surfaces is an important sink of NO_x, especially at night and in winter with relatively weak photochemistry. The uptake coefficient of N_2O_5 depends on aerosol types and meteorological conditions, as parameterized in the current GEOS-Chem (Evans and Jacob, 2005). More recent lab experiments suggested the coefficient to be lower than the Evans and Jacob (2005) estimate by a factor of up to 10 with dependence on meteorological conditions that is still not clear (Bertram et al., 2009; Brown et al., 2009). A sensitivity simulation reduces the uptake coefficient by an order of magnitude (Case 29 in Table 1). It consequently increases model NO_2 columns by 0–6 % over most regions in July and by more than 50 % over part of the northwest in January (Fig. 10e, f). The results are consistent with Lin and McElroy (2011).

5.5 Aerosol optical properties

The tropospheric photochemistry is affected by the amount of solar radiation scattered or absorbed by aerosols. Figures S14 and S15 compare modeled AOD with MODIS/Aqua measurements. In July, GEOS-Chem underestimates the MODIS AOD by 10–50 % in many areas of East China (Fig. S14). This is in part because the formation of secondary organic aerosols is not accounted for with the current model setup. For January, however, the CTM overestimates MODIS AOD by more than 100 % in many places (Fig. S15). Further research is required to fully understand the causes of these differences.

Two test simulations are performed here to quantify the impacts of aerosol scattering and absorption on model NO_2 columns. The first test turns off both scattering and absorption of aerosols in calculating the photochemistry (Case 30 in Table 1). It thus increases model NO_2 columns in July by 0–6 % over most regions but has a negative impact of 10–20 % in January for a large portion of East China (Fig. 11a, b). Another test turns off the effect of black carbon alone resulting in reductions of NO_2 by 0–6 % in July and by up to 20 % in January (Case 31 in Table 1; Fig. 11c, d). The differences (magnitude and sign) are evident between the two tests and between the two months. It is because most aerosols and NO_x are collocated in the PBL, in which situation scattering by aerosols alone tends to increase the actinic flux for photodissociation of

NO_2 while absorption by aerosols decreases the actinic flux. In July, the amount of black carbon (emitted mostly from the residential sector) is small relative to scattering aerosols, resulting in a dominant effect by scattering. In January, the concentration of black carbon increases; thus the aerosol scattering enhances the effect of absorption by providing more diffuse radiation, resulting in enhanced reduction of the actinic flux.

5.6 Emissions

Emissions of CO and (to a lesser extent) SO_2 affect the OH content with consequences on the reaction of OH and NO_2 and other related photochemical processes. Large uncertainties, however, exist in current emission estimates based on both bottom-up and top-down approaches (Fortems-Cheiney et al., 2011; Lu et al., 2011). Here a test simulation is performed to evaluate the impact of emissions of CO and SO_2 on model NO_2 columns, by increasing their emissions by 50 % (Case 32 in Table 1). It thus enhances the NO_2 columns by up to 6 % over North China in July and by up to 10 % over the south in January (Fig. S16a, b).

Emissions of VOC affect OH and other radicals with consequences on the formation of HNO_3 and organic nitrates. Recent ground- and space-based measurements have suggested anthropogenic emissions of aromatics to be underestimated by a factor of 4–10 over East China in the INTEX-B inventory employed here (Liu et al., 2010, 2011). Meanwhile, the current model setup does not include the simulation of aromatics, preventing a direct evaluation of their impacts on model NO_2 columns. Analysis on propene and aromatics, however, suggests similarity in reactivity and oxidation products with respect to OH, pointing to a possibility of using propene as a proxy of aromatics in the model for purposes of sensitivity evaluation. Based on the reactivity and emission strength (provided from INTEX-B), it is estimated that assuming an extra source (50 %) of propene can roughly represent the effect of aromatics on the nitrogen chemistry in accordance with the emission inventory. Therefore two tests are performed here to indirectly evaluate the impact of aromatics on model NO_2 columns, by increasing emissions of propene by 50 % and 300 % (i.e., assuming emissions of aromatics to be six times as much as INTEX-B), respectively (Cases 33–34 in Table 1). The 50 % increase in propene emissions results in small changes (i.e., within 2 %) in model NO_2 columns for both months (Fig. S16c, d). Increasing emissions of propene by 300 % enhances the NO_2 columns by 0–4 % over most regions in July with a negative effect of 0–20 % in most areas in January (Fig. 12). The different signs and magnitudes of NO_2 changes in the two months are attributed mainly to enhanced formation of PAN compensated by the effect of reduced production of HNO_3 through the $NO_2 + OH$ reaction.

A further simulation increases emissions of CO, SO_2 and VOC together by 50 %, following Lin et al. (2010b) (Case 35 in Table 1). As a result, model NO_2 columns in July increase by up to 6 % over North China but decrease by up to 20 % over the southwest (Fig. S16g). The reduction in the southwest is attributed mainly to the increased formation of organic nitrates. In January, changes in model NO_2 columns are within 4 % over most regions (Fig. S16h).

Emissions of NO_x assumed in GEOS-Chem may also affect the lifetime of NO_x and its partitioning into NO and NO_2 through the nonlinear chemical process. This effect has been estimated to be within 10 % for both January and July on the regional mean basis (Martin et al., 2006; Lin and McElroy, 2011; Lin, 2012).

5.7 Other mechanisms and issues

Several new mechanisms have been proposed in recent years that may also affect the abundances of NO_x in the troposphere. Li et al. (2008, 2009) suggested a reaction of NO_2, excited by solar radiation > 420 nm, with water vapor to produce OH and nitrous acid (HONO). The reaction was estimated to be important at high solar zenith angles with low OH content, i.e., at twilight and/or at high latitudes. However, Carr et al. (2009) suggested a much smaller rate constant and thus negligible impacts on the tropospheric chemistry. The contradiction does not allow for conclusive determination of the true importance of the reaction (Sander et al., 2011). A recent study by Su et al. (2011) suggested a significant source of HONO from soil nitrites, particularly from fertilized soils at low pH values. The subsequent photolysis of HONO leads to production of

Title Page
Abstract Introduction
Conclusions References
Tables Figures
◀▮ ▶▮
◀ ▶
Back Close
Full Screen / Esc
Printer-friendly Version
Interactive Discussion

NO and OH, enhancing both source and sink of NO_x likely with a small net impact on its abundance in the troposphere. Karl et al. (2010) suggested dry deposition of oxygenated VOC to be much larger than normally assumed over deciduous ecosystems. They suggested a consequent enhancement of OH by 0–4 % with a reduction of ozone by 1–3.5 % over East China above the continental surface layer in September. The resulting impacts on model NO_2 columns are expected to be relatively small on the regional scale. Given the large uncertainties, these mechanisms are not included in most CTMs and are not evaluated quantitatively here.

Valin et al. (2011) suggested a potentially significant non-linear effect of model horizontal resolution on simulations of NO_2 due to the interaction between NO_x and HO_x, based on chemical mechanism arguments and 7 days of WRF-Chem simulations (1–7 July, 2006). The effect is highly location and time dependent as affected by the varying meteorological and chemical conditions. It is expected to be smaller in winter (with lengthened lifetime and enhanced horizontal homogeneity of NO_x loosening the requirement on model resolution) than in summer. Vertical resolution may also be important for nitrogen simulations considering the large vertical gradient of NO_x and other related species (Lin and McElroy, 2010). Further research is needed to fully quantify the resolution-induced model errors.

6 Modifying model NO_2 columns accounting for errors in meteorology and chemistry

Model NO_2 columns can be modified on the first order by linearizing the impacts of errors in meteorological and chemical parameters:

$$\begin{aligned}\ln(\Omega) &= f(P_i), \qquad i = 1,2,3,\ldots\\ &\approx \ln\Omega_0 + \sum(\partial\ln\Omega/\partial P_i\cdot\Delta P_i)\\ \Rightarrow \Omega &= \Omega_0\cdot\exp^{\sum(\partial\ln\Omega/\partial P_i\cdot\Delta P_i)} \qquad (1)\end{aligned}$$

where Ω represents the post-modification NO_2 columns, Ω_0 represents modeled NO_2 columns prior to the modifications, P_i represents a particular meteorological or chemical parameter, and $f(P_i)$ represents the CTM. $\partial\ln\Omega/\partial P_i$ is derived from the sensitivity simulations, and ΔP_i is the quantified errors of the given parameter based on current knowledge. The modifications are done for gridboxes (at 0.25° long × 0.25° lat) with respect to the 284 ground meteorological stations, assuming that the impacts are local for NO_2 columns. To partially account for the effect of horizontal transport, the NO_2 columns are smoothed with values from the surrounding eight gridboxes (i.e., 3 gridboxes by 3 gridboxes smoothing) prior to the modifications.

Parameters considered for post-model modification include air temperature, water vapor content, COD, uptake coefficients on aerosols for HO_2 and N_2O_5, rate constant for reaction of OH and NO_2, OH regeneration from the isoprene chemistry, net yield of isoprene nitrates, aromatics (as represented by the 300 % increase in propene emissions), and scattering and absorption of radiation by aerosols (see Table 2). Potential errors in modeled PBL mixing are not accounted for here in lack of adequate measurements; the likely underestimate in the nighttime PBLH only has a small impact on modeled NO_2 columns in the afternoon (Fig. 6c, d; see Sect. 4.4). Errors in emissions of CO and SO_2 are also not taken into account due to lack of adequate information (Fortems-Cheiney et al., 2011; Lu et al., 2011). Errors in NO_x emissions may affect modeling of the non-linear photochemistry (see Sect. 5.6); they are however not accounted for in this section aiming to evaluate the model performance with a given amount of NO_x emissions.

As detailed in Table 2, the observed meteorological parameters are taken from the ISH and ISCCP datasets for parameter error calculations. The modeled effect of aerosol scattering and absorption is adjusted based on the comparison between model and MODIS AOD. The best estimate rate constant for OH + NO_2 reaction is taken to be 15 % lower than adopted in the CTM (Mollner et al., 2010; Sander et al., 2011). The net yield of isoprene nitrates is best estimated at 6 % instead of 10 % (Paulot et al., 2009), neglecting for simplicity the horizontal transport of isoprene nitrates affecting the spatial distribution of NO_x. The uptake coefficient of N_2O_5 on aerosols is taken to be 10 % of the value adopted in GEOS-Chem (Bertram et al., 2009; Brown et al., 2009) as a highly simplified modification. A more appropriate value of 0.2 is assumed for the uptake coefficient of HO_2 to account for the large amount of TMIs in China (He et al., 2001; Thornton et al., 2008; Yang et al., 2011), as a rough estimate. In analyzing the uptake of HO_2 and N_2O_5, the surface areas of aerosols are scaled by the ratio of MODIS AOD to model values. Note that these simplified modifications serve only to infer the impacts of potential errors in model meteorology and chemistry; and they cannot be interpreted literally as true apportionment of model errors.

Table 2 and Figs. 13, 14 compare the NO_2 columns with and without post-model modifications. Figures 13, 14 also present results of the RMA regression for NO_2 columns pre- and post-modifications. Modification accounting for the uptake coefficient of HO_2 on aerosols has the largest impact on NO_2 columns across East China, resulting in a slope of about 1.16 in July and 1.10 in January (Figs. 13g, 14g). Modification for COD also has a large impact in July with a slope of about 1.12 (Fig. 13c). Medications for the rate constant of OH + NO_2 reaction and the approximate representation of aromatics using propene have important consequences in July and January, respectively (Figs. 13d, 14i).

Taking into account all modifications, the resulting NO_2 columns are highly correlated with the values prior to the modifications (Figs. 13a, 14a). They however are larger than model values in most places with a slope of about 1.39 in July and 1.09 for January under the RMA regression (Figs. 13a, 14a). Averaged over the stations, all modifications combined increase the NO_2 columns by 22 % in July and by 10 % in January. This suggests significant systematic biases in GEOS-Chem with important consequences on the inverse modeling of NO_x emissions and other related applications. That model errors are likely larger in summer than in winter is in broad consistency with the findings of Huijnen et al. (2010) for Europe.

van Noije et al. (2006) compared NO_2 columns for 2000 simulated by nine global models differing in spatial resolution, meteorological inputs, soil/lightning emissions, uptake of N_2O_5 on aerosols and other gaseous and heterogeneous chemical mechanisms. They found results for both July and January over Eastern China (110°–123° E, 30°–40° N) from three models to be different by up to 50 % from six other models providing more consistent simulations (including GEOS-Chem). van Noijie et al. (2006) also found large inter-model spread in Europe, as confirmed by Huijnen et al. (2010) evaluating eight regional models and two global models. The inter-model differences in simulated NO_2 columns are likely because errors in meteorological/chemical parameters are inconsistent in sign and/or magnitude across the models. For example, parameters and processes may be overestimated by some models but neglected/underestimated by other models.

Note that the modified columns are still lower than satellite retrievals with a slope of about 0.68 in July and 0.54 in January (Fig. 2c, d). The negative biases are driven mainly by those in polluted areas with retrieved NO_2 columns exceeding 6×10^{15} molecules cm^{-2} in July and 12×10^{15} molecules cm^{-2} in January. For cleaner areas, the slope increases to about 1.06 in July and 0.91 in January.

7 Implications for surface ozone simulation of errors in model meteorological and chemical parameters

Errors in model meteorology and chemistry also have significant impacts on simulations of surface ozone. Here the post-model modification (as done for NO_2 in Sect. 6) is implemented to simulated ozone concentrations to evaluate the respective model performance. Results are presented in Table 2 and Figs. 15, 16. They should be interpreted with caution since the effect of horizontal transport is not fully taken into account by the localized station-by-station adjustments, in addition to the linearization assumption and simplified error quantification for model parameters.

Modification accounting for the uptake coefficient of HO_2 on aerosols has the largest impact on surface ozone. In July, it results in a slope of 0.93 with a R^2 of 0.89 from the RMA regression (Fig. 15g). More importantly, it reduces the peak ozone concentration by about 15 ppb. The large sensitivity of O_3 formation to HO_2 uptake efficiency was also found by recent observation-based modeling studies over the region (Kanaya, et al., 2009; Liu et al., 2012). In January, the impacts are more location-dependent with the R^2 decreasing to about 0.71 (Fig. 16g). Modifications for COD and aromatics (represented by propene) also have significant consequences on surface ozone in January, followed by modifications for AOD and water vapor (Fig. 16b, c, i, j). For July, modifications are important on temperature, water vapor, COD and aromatics (Fig. 15a, b, c, i).

All modifications combined result in a slope of about 0.86 with an intercept of 7.4 ppb in July for surface ozone (Fig. 15a). Spatially, ozone concentrations are reduced in the north but enhanced in the south resulting in a R^2 of about 0.82 (Fig. 15a). For January, ozone concentrations are decreased in the west but increased in the east resulting in a weak spatial correlation with a R^2 of 0.22 only (Fig. 16a). The spatial pattern is attributed primarily to the negative impacts of modifications for COD and HO_2 uptake coefficient counteracted by the positive effect of inclusion of aromatics (represented by increased propene emissions).

8 Conclusions

Satellite remote sensing has been proven useful in constraining emissions of NO_x, particularly for China and other developing countries for which bottom-up inventories contain large uncertainties and/or are not updated timely to reflect the rapid emission growth. Such top-down constraint is subject to errors not just in satellite retrievals but also in model simulations interpreting the relation between observed abundance of nitrogen and its emissions. Quantifying the model errors over China is however challenging due to lack of sufficient in-situ measurements of nitrogen. In this study, an alternate approach is proposed for model evaluation over East China by conducting a systematic analysis of meteorological and chemical parameters affecting the simulation of NO_x. The analysis is focused in January and July 2006 to evaluate the seasonal dependence of model sensitivity to meteorology and chemistry.

As a demonstration, the nested version for Asia of the widely used GEOS-Chem model is evaluated here. The CTM is driven by the GEOS-5 meteorological fields and the INTEX-B anthropogenic emissions for Asia, as used in the inverse modeling of NO_x emissions and many other applications (Lin et al., 2010a,b; Lin and McElroy, 2010, 2011; Lin, 2012; Wang et al., 2012) (see also http://acmg.seas.harvard.edu/recentpapers.html). The nested model has been found to underestimate NO_2 columns retrieved from OMI (DOMINO-2) by about 20 % in July and by as large as 36 % in January averaged over East China (Lin, 2012). Modeled NO_2 columns are only about 20–30 % of retrieved values over extremely polluted areas such as cities and those with large point sources, particular in the north in January (Lin, 2012).

Errors in the GEOS-5 meteorological fields are evaluated with observations from the ground network (NCDC ISH) and from space (ISCCP). GEOS-5 significantly underestimates cloud fraction and cloud optical depth over East China as compared to measurements from ISCCP. It also contains errors of regional and seasonal dependence in air temperature, relative humidity, water vapor content, wind speed and precipitation. Sensitivity simulations suggest that the impacts of these errors on modeled NO_2 columns are normally below 20 % across East China.

Errors in PBL mixing affecting the vertical distribution of NO_2 are difficult to quantify due to lack of direct observations. A series of sensitivity simulations perturbing the PBLH show significant influences on model NO_2 columns (when the averaging kernel from the satellite product is applied to simulated vertical distribution of NO_2). A 100 % increase in PBLH results in closer agreement between modeled and retrieved columns averaged over East China; it however cannot eliminate the negative biases in extremely polluted areas.

A variety of chemical parameters are also evaluated with the CTM based on current understanding of their uncertainties. Factors considered include the rate constant for reaction of $OH + NO_2$, yield of HNO_3 from reaction of $NO + HO_2$, OH regeneration from the isoprene chemistry, yield and fate of isoprene nitrates, equilibrium constant for formation and thermal decomposition of PAN, uptake coefficients on aerosols for HO_2 and N_2O_5, chemistry of aromatics, emissions of CO, VOC and SO_2, and scattering and absorption of solar radiation by aerosols. Perturbations on these factors affect simulated NO_2 columns by various magnitudes strongly depending on regions and seasons.

Attempts are made to modify the columns simulated at the 284 ground meteorological stations in East China, accounting for errors in various meteorological and chemical parameters. The modifications together increase the NO_2 columns by 22 % in July and by 10 % in January averaged across the stations, likely indicating systematic model errors. They result in closer agreement with satellite retrievals, but cannot eliminate the negative biases in extremely polluted places. Individually, assuming the uptake coefficient of HO_2 on aerosols to be 0.2 (to account for the large amount of transition metal ions) has the largest impact on NO_2 columns, followed by corrections on COD, rate constant of $OH + NO_2$ reaction, uptake coefficient of N_2O_5 on aerosols, and inclusion of aromatics.

Errors in meteorological and chemical parameters also have significant consequences on simulations of ozone and its regional and global transport. A similar post-model modification for surface ozone in July results in decreases of ozone concentrations in the north with increases in the south, both by about 0–20 %. In particular, the peak values are reduced by about 15 ppb. For January, ozone concentrations are reduced in the west and enhanced in the east, with the differences exceeding 20 % in many places.

It is important to understand the large differences between modeled and retrieved tropospheric NO_2 columns in extremely polluted areas. Model errors appear not to be the primary cause based on the present analysis. Satellite retrievals are sensitive to assumptions on the amount of stratospheric NO_2, aerosols, clouds, surface reflectance, terrain height, and a priori vertical profile of NO_2. Most aerosols of anthropogenic origin are collocated with NO_2 in the PBL, affecting the amount of solar radiation absorbed by NO_2. The presence of aerosols is not accounted for explicitly in current satellite NO_2 products; and their scattering effect is treated implicitly with arbitrarily enhanced cloud fraction. The sensitivity of NO_2 columns on aerosol scattering and absorption is found in this study to be within 20 % across East China, a value much smaller than the magnitude of model underestimation in extremely polluted areas. The presence of aerosols may also affect the retrieval of surface reflectance with consequences on subsequent cloud and NO_2 retrievals. This factor cannot likely account for the large model underestimation in extremely polluted areas. In addition, errors (in percentage) in satellite retrievals caused by non-aerosol factors are not expected to be highly correlated to the amount of NO_2. Therefore retrieval errors seem unlikely to be the main source of model-retrieval differences in extremely polluted areas. It appears that the differences are derived more likely from the underestimate of NO_x emissions in the INTEX-B inventory used to drive the model simulations.

Supplementary material related to this article is available online at: http://www.atmos-chem-phys-discuss.net/12/14269/2012/acpd-12-14269-2012-supplement.pdf.

Acknowledgements. This research is supported by the National Natural Science Foundation of China, grant 41005078 and 41175127. The work of G. Zhuang is supported by the great international collaboration project of MOST, China (2010DFA92230), National Natural Science Foundation of China (Grant No. 41128005, fund for collaboration with oversea scholars). We acknowledge the free use of tropospheric NO_2 column data from www.temis.nl, MODIS AOD data from NASA, and meteorological data from NOAA NCDC and the ISCCP project. We thank Randall V. Martin and Mathew Evans for useful comments.

References

van der A, R. J., Peters, D., Eskes, H., Boersma, K. F., Van Roozendael, M., De Smedt, I., and Kelder, H. M.: Detection of the trend and seasonal variation in tropospheric NO_2 over China, J. Geophys. Res.-Atmos., 111, D12317, doi:10.1029/2005jd006594, 2006.

Atkinson, R., Baulch, D. L., Cox, R. A., Crowley, J. N., Hampson, R. F., Hynes, R. G., Jenkin, M. E., Rossi, M. J., and Troe, J.: Evaluated kinetic and photochemical data for atmospheric chemistry: Volume I – gas phase reactions of O_x, HO_x, NO_x and SO_x species, Atmos. Chem. Phys., 4, 1461–1738, doi:10.5194/acp-4-1461-2004, 2004.

Atkinson, R., Baulch, D. L., Cox, R. A., Crowley, J. N., Hampson, R. F., Hynes, R. G., Jenkin, M. E., Rossi, M. J., Troe, J., and IUPAC Subcommittee: Evaluated kinetic and photochemical data for atmospheric chemistry: Volume II – gas phase reactions of organic species, Atmos. Chem. Phys., 6, 3625–4055, doi:10.5194/acp-6-3625-2006, 2006.

Bertram, T. H., Thornton, J. A., Riedel, T. P., Middlebrook, A. M., Bahreini, R., Bates, T. S., Quinn, P. K., and Coffman, D. J.: Direct observations of N_2O_5 reactivity on ambient aerosol particles, Geophys. Res. Lett., 36, L19803, doi:10.1029/2009gl040248, 2009.

Boersma, K. F., Jacob, D. J., Trainic, M., Rudich, Y., DeSmedt, I., Dirksen, R., and Eskes, H. J.: Validation of urban NO_2 concentrations and their diurnal and seasonal variations observed from the SCIAMACHY and OMI sensors using in situ surface measurements in Israeli cities, Atmos. Chem. Phys., 9, 3867–3879, doi:10.5194/acp-9-3867-2009, 2009.

Boersma, K. F., Jacob, D. J., Bucsela, E. J., Perring, A. E., Dirksen, R., van der A, R. J., Yantosca, R. M., Park, R. J., Wenig, M. O., Bertram, T. H., and Cohen, R. C.: Validation of OMI tropospheric NO_2 observations during INTEX-B and application to constrain NO_x emissions over the Eastern United States and Mexico, Atmos. Environ., 42, 4480–4497, doi:10.1016/j.atmosenv.2008.02.004, 2008.

Boersma, K. F., Eskes, H. J., Dirksen, R. J., van der A, R. J., Veefkind, J. P., Stammes, P., Huijnen, V., Kleipool, Q. L., Sneep, M., Claas, J., Leitão, J., Richter, A., Zhou, Y., and Brunner, D.: An improved tropospheric NO_2 column retrieval algorithm for the Ozone Monitoring Instrument, Atmos. Meas. Tech., 4, 1905–1928, doi:10.5194/amt-4-1905-2011, 2011.

Brinksma, E. J., Pinardi, G., Volten, H., Braak, R., Richter, A., Schonhardt, A., van Roozendael, M., Fayt, C., Hermans, C., Dirksen, R. J., Vlemmix, T., Berkhout, A. J. C., Swart, D. P. J., Oetjen, H., Wittrock, F., Wagner, T., Ibrahim, O. W., de Leeuw, G., Moerman, M., Curier, R. L., Celarier, E. A., Cede, A., Knap, W. H., Veefkind, J. P., Eskes, H. J., Allaart, M., Rothe, R., Piters, A. J. M., and Levelt, P. F.: The 2005 and 2006 DANDELIONS NO_2 and aerosol intercomparison campaigns, J. Geophys. Res.-Atmos., 113, D16S46, doi:10.1029/2007jd008808, 2008.

Brown, S. S., Dube, W. P., Fuchs, H., Ryerson, T. B., Wollny, A. G., Brock, C. A., Bahreini, R., Middlebrook, A. M., Neuman, J. A., Atlas, E., Roberts, J. M., Osthoff, H. D., Trainer, M., Fehsenfeld, F. C., and Ravishankara, A. R.: Reactive uptake coefficients for N_2O_5 determined from aircraft measurements during the Second Texas Air Quality Study: comparison to current model parameterizations, J. Geophys. Res.-Atmos., 114, D00F10, doi:10.1029/2008jd011679, 2009.

Bucsela, E. J., Perring, A. E., Cohen, R. C., Boersma, K. F., Celarier, E. A., Gleason, J. F., Wenig, M. O., Bertram, T. H., Wooldridge, P. J., Dirksen, R., and Veefkind, J. P.: Comparison of tropospheric NO_2 from in situ aircraft measurements with near-real-time and standard product data from OMI, J. Geophys. Res.-Atmos., 113, D16S31, doi:10.1029/2007jd008838, 2008.

Butkovskaya, N., Kukui, A., and Le Bras, G.: HNO_3 forming channel of the $HO_2 + NO$ reaction as a function of pressure and temperature in the ranges of 72–600 torr and 223–323 K, J. Phys. Chem. A, 111, 9047–9053, doi:10.1021/jp074117m, 2007.

Butkovskaya, N., Rayez, M.-T., Rayez, J.-C., Kukui, A., and Le Bras, G.: Water vapor effect on the HNO_3 yield in the $HO_2 + NO$ reaction: experimental and theoretical evidence, J. Phys. Chem. A, 113, 11327–11342, doi:10.1021/jp811428p, 2009.

Butkovskaya, N. I., Kukui, A., Pouvesle, N., and Le Bras, G.: Formation of nitric acid in the gas-phase $HO_2 + NO$ reaction: effects of temperature and water vapor, J. Phys. Chem. A, 109, 6509–6520, doi:10.1021/jp051534v, 2005.

Butler, T. M., Taraborrelli, D., Brühl, C., Fischer, H., Harder, H., Martinez, M., Williams, J., Lawrence, M. G., and Lelieveld, J.: Improved simulation of isoprene oxidation chemistry with the ECHAM5/MESSy chemistry-climate model: lessons from the GABRIEL airborne field campaign, Atmos. Chem. Phys., 8, 4529–4546, doi:10.5194/acp-8-4529-2008, 2008.

Carr, S., Heard, D. E., and Blitz, M. A.: Comment on "Atmospheric hydroxyl radical production from electronically excited NO_2 and H_2O", Science, 324, p. 336, doi:10.1126/science.1166669, 2009.

Chen, D., Wang, Y., McElroy, M. B., He, K., Yantosca, R. M., and Le Sager, P.: Regional CO pollution and export in China simulated by the high-resolution nested-grid GEOS-Chem model, Atmos. Chem. Phys., 9, 3825–3839, doi:10.5194/acp-9-3825-2009, 2009.

Chen, X. H., Hulbert, D., and Shepson, P. B.: Measurement of the organic nitrate yield from OH reaction with isoprene, J. Geophys. Res.-Atmos., 103, 25563–25568, doi:10.1029/98jd01483, 1998.

Emmerson, K. M. and Evans, M. J.: Comparison of tropospheric gas-phase chemistry schemes for use within global models, Atmos. Chem. Phys., 9, 1831–1845, doi:10.5194/acp-9-1831-2009, 2009.

Evans, M. J. and Jacob, D. J.: Impact of new laboratory studies of N_2O_5 hydrolysis on global model budgets of tropospheric nitrogen oxides, ozone, and OH, Geophys. Res. Lett., 32, L09813, doi:10.1029/2005gl022469, 2005.

Fiore, A. M., Horowitz, L. W., Purves, D. W., Levy, H., Evans, M. J., Wang, Y. X., Li, Q. B., and Yantosca, R. M.: Evaluating the contribution of changes in isoprene emissions to surface ozone trends over the Eastern United States, J. Geophys. Res.-Atmos., 110, D12303, doi:10.1029/2004jd005485, 2005.

Fortems-Cheiney, A., Chevallier, F., Pison, I., Bousquet, P., Szopa, S., Deeter, M. N., and Clerbaux, C.: Ten years of CO emissions as seen from Measurements of Pollution in the Troposphere (MOPITT), J. Geophys. Res.-Atmos., 116, D05304, doi:10.1029/2010jd014416, 2011.

Global Modeling and Assimilation Office: File Specification for GEOS-5 DAS Gridded Output Document No. GMAO-1001v6.1, Global Modeling and Assimilation Office, Earth Sciences Division NASA Goddard Space Flight Center, Greenbelt, Maryland 20771, 2006.

He, K. B., Yang, F. M., Ma, Y. L., Zhang, Q., Yao, X. H., Chan, C. K., Cadle, S., Chan, T., and Mulawa, P.: The characteristics of $PM_{2.5}$ in Beijing, China, Atmos. Environ., 35, 4959–4970, 2001.

Holtslag, A. and Boville, B.: Local versus nonlocal boundary-layer diffusion in a global climate model, J. Climate, 6, 1825–1842, 1993.

Horowitz, L. W., Fiore, A. M., Milly, G. P., Cohen, R. C., Perring, A., Wooldridge, P. J., Hess, P. G., Emmons, L. K., and Lamarque, J.-F.: Observational constraints on the chemistry of isoprene nitrates over the Eastern United States, J. Geophys. Res.-Atmos., 112, D12S08, doi:10.1029/2006jd007747, 2007.

Horowitz, L. W., Walters, S., Mauzerall, D. L., Emmons, L. K., Rasch, P. J., Granier, C., Tie, X. X., Lamarque, J. F., Schultz, M. G., Tyndall, G. S., Orlando, J. J., and Brasseur, G. P.: A global simulation of tropospheric ozone and related tracers: description and evaluation of MOZART, version 2, J. Geophys. Res.-Atmos., 108, 4784–4508, doi:10.1029/2002jd002853, 2003.

Hudman, R. C., Jacob, D. J., Turquety, S., Leibensperger, E. M., Murray, L. T., Wu, S., Gilliland, A. B., Avery, M., Bertram, T. H., Brune, W., Cohen, R. C., Dibb, J. E., Flocke, F. M., Fried, A., Holloway, J., Neuman, J. A., Orville, R., Perring, A., Ren, X., Sachse, G. W., Singh, H. B., Swanson, A., and Wooldridge, P. J.: Surface and lightning sources of nitrogen oxides over the United States: magnitudes, chemical evolution, and outflow, J. Geophys. Res.-Atmos., 112, D12S05, doi:10.1029/2006jd007912, 2007.

Huijnen, V., Eskes, H. J., Poupkou, A., Elbern, H., Boersma, K. F., Foret, G., Sofiev, M., Valdebenito, A., Flemming, J., Stein, O., Gross, A., Robertson, L., D'Isidoro, M., Kioutsioukis, I., Friese, E., Amstrup, B., Bergstrom, R., Strunk, A., Vira, J., Zyryanov, D., Maurizi, A., Melas, D., Peuch, V.-H., and Zerefos, C.: Comparison of OMI NO_2 tropospheric columns with an ensemble of global and European regional air quality models, Atmos. Chem. Phys., 10, 3273–3296, doi:10.5194/acp-10-3273-2010, 2010.

Ito, A., Sillman, S., and Penner, J. E.: Global chemical transport model study of ozone response to changes in chemical kinetics and biogenic volatile organic compounds emissions due to increasing temperatures: sensitivities to isoprene nitrate chemistry and grid resolution, J. Geophys. Res.-Atmos., 114, D09301, doi:10.1029/2008jd011254, 2009.

Jacob, D. J.: Heterogeneous chemistry and tropospheric ozone, Atmos. Environ., 34, 2131–2159, doi:10.1016/s1352-2310(99)00462-8, 2000.

Jaeglé, L., Steinberger, L., Martin, R. V., and Chance, K.: Global partitioning of NO_x sources using satellite observations: Relative roles of fossil fuel combustion, biomass burning and soil emissions, Faraday Discuss., 130, 407–423, doi:10.1039/b502128f, 2005.

Kanaya, Y., Pochanart, P., Liu, Y., Li, J., Tanimoto, H., Kato, S., Suthawaree, J., Inomata, S., Taketani, F., Okuzawa, K., Kawamura, K., Akimoto, H., and Wang, Z. F.: Rates and regimes of photochemical ozone production over Central East China in June 2006: a box model analysis using comprehensive measurements of ozone precursors, Atmos. Chem. Phys., 9, 7711–7723, doi:10.5194/acp-9-7711-2009, 2009.

Karl, T., Harley, P., Emmons, L., Thornton, B., Guenther, A., Basu, C., Turnipseed, A., and Jardine, K.: Efficient Atmospheric Cleansing of Oxidized Organic Trace Gases by Vegetation, Science, 330, 816–819, doi:10.1126/science.1192534, 2010.

Kolb, C. E., Cox, R. A., Abbatt, J. P. D., Ammann, M., Davis, E. J., Donaldson, D. J., Garrett, B. C., George, C., Griffiths, P. T., Hanson, D. R., Kulmala, M., McFiggans, G., Pöschl, U., Riipinen, I., Rossi, M. J., Rudich, Y., Wagner, P. E., Winkler, P. M., Worsnop, D. R., and O' Dowd, C. D.: An overview of current issues in the uptake of atmospheric trace gases by aerosols and clouds, Atmos. Chem. Phys., 10, 10561–10605, doi:10.5194/acp-10-10561-2010, 2010.

Kubistin, D., Harder, H., Martinez, M., Rudolf, M., Sander, R., Bozem, H., Eerdekens, G., Fischer, H., Gurk, C., Klüpfel, T., Königstedt, R., Parchatka, U., Schiller, C. L., Stickler, A., Taraborrelli, D., Williams, J., and Lelieveld, J.: Hydroxyl radicals in the tropical troposphere over the Suriname rainforest: comparison of measurements with the box model MECCA, Atmos. Chem. Phys., 10, 9705–9728, doi:10.5194/acp-10-9705-2010, 2010.

Lamsal, L. N., Martin, R. V., van Donkelaar, A., Celarier, E. A., Bucsela, E. J., Boersma, K. F., Dirksen, R., Luo, C., and Wang, Y.: Indirect validation of tropospheric nitrogen dioxide retrieved from the OMI satellite instrument: insight into the seasonal variation of nitrogen oxides at northern midlatitudes, J. Geophys. Res.-Atmos., 115, D05302, doi:10.1029/2009jd013351, 2010.

Lamsal, L. N., Martin, R. V., Padmanabhan, A., van Donkelaar, A., Zhang, Q., Sioris, C. E., Chance, K., Kurosu, T. P., and Newchurch, M. J.: Application of satellite observations for timely updates to global anthropogenic NO_x emission inventories, Geophys. Res. Lett., 38, L05810, doi:10.1029/2010gl046476, 2011.

Lelieveld, J., Butler, T. M., Crowley, J. N., Dillon, T. J., Fischer, H., Ganzeveld, L., Harder, H., Lawrence, M. G., Martinez, M., Taraborrelli, D., and Williams, J.: Atmospheric oxidation capacity sustained by a tropical forest, Nature, 452, 737–740, doi:10.1038/nature06870, 2008.

Li, S., Matthews, J., and Sinha, A.: Atmospheric hydroxyl radical production from electronically excited NO_2 and H_2O, Science, 319, 1657–1660, doi:10.1126/science.1151443, 2008.

Li, S., Matthews, J., and Sinha, A.: Response to Comment on "Atmospheric hydroxyl radical production from electronically excited NO_2 and H_2O", Science, 324, p. 336, doi:10.1126/science.1166877, 2009.

Lin, J.-T.: Satellite constraint for emissions of nitrogen oxides from anthropogenic, lightning and soil sources over East China on a high-resolution grid, Atmos. Chem. Phys., 12, 2881–2898, doi:10.5194/acp-12-2881-2012, 2012.

Lin, J. T. and McElroy, M. B.: Impacts of boundary layer mixing on pollutant vertical profiles in the lower troposphere: implications to satellite remote sensing, Atmos. Environ., 44, 1726–1739, doi:10.1016/j.atmosenv.2010.02.009, 2010.

Lin, J.-T. and McElroy, M. B.: Detection from space of a reduction in anthropogenic emissions of nitrogen oxides during the Chinese economic downturn, Atmos. Chem. Phys., 11, 8171–8188, doi:10.5194/acp-11-8171-2011, 2011.

Lin, J.-T., Liang, X.-Z., and Wuebbles, D. J.: Effects of intercontinental transport on surface ozone over the United States: present and future assessment with a global model, Geophys. Res. Lett., 35, L02805, doi:10.1029/2007GL031415, 2008a.

Lin, J.-T., Youn, D., Liang, X.-Z., and Wuebbles, D. J.: Global model simulation of summertime US ozone diurnal cycle and its sensitivity to PBL mixing, spatial resolution, and emissions, Atmos. Environ., 42, 8470–8483, doi:10.1016/j.atmosenv.2008.08.012, 2008b.

Lin, J.-T., Patten, K. O., Hayhoe, K., Liang, X.-Z., and Wuebbles, D. J.: Effects of future climate and biogenic emission changes on surface ozone over the United States and China, J. Appl. Meteor., 47, 1888–1909, doi:10.1175/2007JAMC1681.1, 2008c.

Lin, J.-T., Nielsen, C. P., Zhao, Y., Lei, Y., Liu, Y., and McElroy, M. B.: Recent changes in particulate air pollution over China observed from space and the ground: effectiveness of emission control, Environ. Sci. Technol., 44, 7771–7776, doi:10.1021/es101094t, 2010a.

Lin, J.-T., McElroy, M. B., and Boersma, K. F.: Constraint of anthropogenic NO_x emissions in China from different sectors: a new methodology using multiple satellite retrievals, Atmos. Chem. Phys., 10, 63–78, doi:10.5194/acp-10-63-2010, 2010b.

Liu, H., Crawford, J. H., Considine, D. B., Platnick, S., Norris, P. M., Duncan, B. N., Pierce, R. B., Gao, C., and Yantosca, R. M.: Sensitivity of photolysis frequencies and key tropospheric oxidants in a global model to cloud vertical distributions and optical properties, J. Geophys. Res., 114, D10305, doi:10.1029/2008jd011503, 2009.

Liu, S. and Liang, X.-Z.: Observed diurnal cycle climatology of planetary boundary layer height, J. Climate, 23, 5790–5809, doi:10.1175/2010jcli3552.1, 2010.

Liu, Z., Wang, Y., Zhao, C., Vrekoussis, M., Richter, A., Wittrock, F., Burrow, J. P., Shao, M., Liu, S.-C., Chang, C.-C., Wang, H., and Chen, C.: The missing source of glyoxal over China and its implications on organic aerosol budgets, AGU Fall Meeting 2011, San Francisco, abstract #A21I-07, 2011.

Liu, Z., Wang, Y., Gu, D., Zhao, C., Huey, L. G., Stickel, R., Liao, J., Shao, M., Zhu, T., Zeng, L., Liu, S.-C., Chang, C.-C., Amoroso, A., and Costabile, F.: Evidence of reactive aromatics as a major source of peroxy acetyl nitrate over China, Environ. Sci. Technol., 44, 7017–7022, doi:10.1021/es1007966, 2010.

Liu, Z., Wang, Y., Gu, D., Zhao, C., Huey, L. G., Stickel, R., Liao, J., Shao, M., Zhu, T., Zeng, L., Amoroso, A., Costabile, F., Chang, C.-C., and Liu, S.-C.: Summertime photochemistry during CAREBeijing-2007: RO_x budgets and O_3 formation, Atmos. Chem. Phys. Discuss., 12, 4679–4717, doi:10.5194/acpd-12-4679-2012, 2012.

Lu, Z., Zhang, Q., and Streets, D. G.: Sulfur dioxide and primary carbonaceous aerosol emissions in China and India, 1996–2010, Atmos. Chem. Phys., 11, 9839–9864, doi:10.5194/acp-11-9839-2011, 2011.

Macintyre, H. L. and Evans, M. J.: Parameterisation and impact of aerosol uptake of HO_2 on a global tropospheric model, Atmos. Chem. Phys., 11, 10965–10974, doi:10.5194/acp-11-10965-2011, 2011.

Mao, J., Jacob, D. J., Evans, M. J., Olson, J. R., Ren, X., Brune, W. H., Clair, J. M. St., Crounse, J. D., Spencer, K. M., Beaver, M. R., Wennberg, P. O., Cubison, M. J., Jimenez, J. L., Fried, A., Weibring, P., Walega, J. G., Hall, S. R., Weinheimer, A. J., Cohen, R. C., Chen, G., Crawford, J. H., McNaughton, C., Clarke, A. D., Jaeglé, L., Fisher, J. A., Yantosca, R. M., Le Sager, P., and Carouge, C.: Chemistry of hydrogen oxide radicals (HO_x) in the Arctic troposphere in spring, Atmos. Chem. Phys., 10, 5823–5838, doi:10.5194/acp-10-5823-2010, 2010.

Martin, R. V., Sioris, C. E., Chance, K., Ryerson, T. B., Bertram, T. H., Wooldridge, P. J., Cohen, R. C., J. Andy Neuman, Swanson, A., and Flocke, F. M.: Evaluation of space-based constraints on global nitrogen oxide emissions with regional aircraft measurements over and downwind of Eastern North America, J. Geophys. Res., 111, D15308, doi:10.1029/2005JD006680, 2006.

Mijling, B., van der A, R. J., Boersma, K. F., Van Roozendael, M., De Smedt, I., and Kelder, H. M.: Reductions of NO_2 detected from space during the 2008 Beijing Olympic Games, Geophys. Res. Lett., 36, L13801, doi:10.1029/2009gl038943, 2009.

Mollner, A. K., Valluvadasan, S., Feng, L., Sprague, M. K., Okumura, M., Milligan, D. B., Bloss, W. J., Sander, S. P., Martien, P. T., Harley, R. A., McCoy, A. B., and Carter, W. P. L.: Rate of gas phase association of hydroxyl radical and nitrogen dioxide, Science, 330, 646–649, doi:10.1126/science.1193030, 2010.

Mao, J., Fan S., and Jacob, D. J.: Radical loss in the atmosphere from Cu-Fe redox coupling in aerosols, Nature, in review, 2012.

van Noije, T. P. C., Eskes, H. J., Dentener, F. J., Stevenson, D. S., Ellingsen, K., Schultz, M. G., Wild, O., Amann, M., Atherton, C. S., Bergmann, D. J., Bey, I., Boersma, K. F., Butler, T., Cofala, J., Drevet, J., Fiore, A. M., Gauss, M., Hauglustaine, D. A., Horowitz, L. W., Isaksen, I. S. A., Krol, M. C., Lamarque, J.-F., Lawrence, M. G., Martin, R. V., Montanaro, V., Müller, J.-F., Pitari, G., Prather, M. J., Pyle, J. A., Richter, A., Rodriguez, J. M., Savage, N. H., Strahan, S. E., Sudo, K., Szopa, S., and van Roozendael, M.: Multi-model ensemble simulations of tropospheric NO_2 compared with GOME retrievals for the year 2000, Atmos. Chem. Phys., 6, 2943–2979, doi:10.5194/acp-6-2943-2006, 2006.

Okumura, M. and Sander, S. P.: Gas-Phase Formation Rates of Nitric Acid and its Isomers under Urban Conditions, State of California Air Resources Board, Sacramento, California 95814, 2005.

Patchen, A. K., Pennino, M. J., Kiep, A. C., and Elrod, M. J.: Direct kinetics study of the product-forming channels of the reaction of isoprene-derived hydroxyperoxy radicals with NO, Int. J. Chem. Kinet., 39, 353–361, doi:10.1002/kin.20248, 2007.

Paulot, F., Crounse, J. D., Kjaergaard, H. G., Kroll, J. H., Seinfeld, J. H., and Wennberg, P. O.: Isoprene photooxidation: new insights into the production of acids and organic nitrates, Atmos. Chem. Phys., 9, 1479–1501, doi:10.5194/acp-9-1479-2009, 2009.

Pryor, S. C. and Barthelmie, R. J.: Assessing climate change impacts on the near-term stability of the wind energy resource over the United States, Proc. Natl. Acad. Sci., 108, 8167–8171, doi:10.1073/pnas.1019388108, 2011.

Richter, A., Burrows, J. P., Nüß, H., Granier, C., and Niemeier, U.: Increase in tropospheric nitrogen dioxide over China observed from space, Nature, 437, 129–132, doi:10.1038/nature04092, 2005.

Sander, S. P., Abbatt, J. P. D., Barker, J. R., Burkholder, J. B., Friedl, R. R., Golden, D. M., Huie, R. E., Kolb, C. E., Kurylo, M. J., Moortgat, G. K., Orkin, V. L., and Wine, P. H.: Chemical Kinetics and Photochemical Data for Use in Atmospheric Studies, JPL Publication 10-06, Pasadena, California, 2011.

Saunders, S. M., Jenkin, M. E., Derwent, R. G., and Pilling, M. J.: Protocol for the development of the Master Chemical Mechanism, MCM v3 (Part A): tropospheric degradation of non-aromatic volatile organic compounds, Atmos. Chem. Phys., 3, 161–180, doi:10.5194/acp-3-161-2003, 2003.

Sauvage, B., Martin, R. V., van Donkelaar, A., Liu, X., Chance, K., Jaeglé, L., Palmer, P. I., Wu, S., and Fu, T.-M.: Remote sensed and in situ constraints on processes affecting tropical tropospheric ozone, Atmos. Chem. Phys., 7, 815–838, doi:10.5194/acp-7-815-2007, 2007.

Singh, H. B., Salas, L., Herlth, D., Kolyer, R., Czech, E., Avery, M., Crawford, J. H., Pierce, R. B., Sachse, G. W., Blake, D. R., Cohen, R. C., Bertram, T. H., Perring, A., Wooldridge, P. J., Dibb, J., Huey, G., Hudman, R. C., Turquety, S., Emmons, L. K., Flocke, F., Tang, Y., Carmichael, G. R., and Horowitz, L. W.: Reactive nitrogen distribution and partitioning in the

North American troposphere and lowermost stratosphere, J. Geophys. Res.-Atmos., 112, D12S04, doi:10.1029/2006jd007664, 2007.

Sprengnether, M., Demerjian, K. L., Donahue, N. M., and Anderson, J. G.: Product analysis of the OH oxidation of isoprene and 1,3-butadiene in the presence of NO, J. Geophys. Res.-Atmos., 107, 4269, doi:10.1029/2001jd000716, 2002.

Stavrakou, T., Muller, J. F., Boersma, K. F., De Smedt, I., and van der A, R. J.: Assessing the distribution and growth rates of NO_x emission sources by inverting a 10-year record of NO_2 satellite columns, Geophys. Res. Lett., 35, L10801, doi:10.1029/2008gl033521, 2008.

Streets, D. G., Bond, T. C., Carmichael, G. R., Fernandes, S. D., Fu, Q., He, D., Klimont, Z., Nelson, S. M., Tsai, N. Y., Wang, M. Q., Woo, J. H., and Yarber, K. F.: An inventory of gaseous and primary aerosol emissions in Asia in the year 2000, J. Geophys. Res.-Atmos., 108, 8809, doi:10.1029/2002jd003093, 2003.

Su, H., Cheng, Y. F., Oswald, R., Behrendt, T., Trebs, I., Meixner, F. X., Andreae, M. O., Cheng, P., Zhang, Y., and Poschl, U.: Soil Nitrite as a Source of Atmospheric HONO and OH Radicals, Science, 333, 1616–1618, doi:10.1126/science.1207687, 2011.

Thornton, J. A., Jaeglé, L., and McNeill, V. F.: Assessing known pathways for HO_2 loss in aqueous atmospheric aerosols: regional and global impacts on tropospheric oxidants, J. Geophys. Res.-Atmos., 113, D05303, doi:10.1029/2007jd009236, 2008.

Tost, H., Lawrence, M. G., Brühl, C., Jöckel, P., The GABRIEL Team, and The SCOUT-O_3-DARWIN/ACTIVE Team: Uncertainties in atmospheric chemistry modelling due to convection parameterisations and subsequent scavenging, Atmos. Chem. Phys., 10, 1931–1951, doi:10.5194/acp-10-1931-2010, 2010.

Valin, L. C., Russell, A. R., Hudman, R. C., and Cohen, R. C.: Effects of model resolution on the interpretation of satellite NO_2 observations, Atmos. Chem. Phys., 11, 11647–11655, doi:10.5194/acp-11-11647-2011, 2011.

Wang, S. W., Zhang, Q., Streets, D. G., He, K. B., Martin, R. V., Lamsal, L. N., Chen, D., Lei, Y., and Lu, Z.: Growth in NO_x emissions from power plants in China: bottom-up estimates and satellite observations, Atmos. Chem. Phys., 12, 4429–4447, doi:10.5194/acp-12-4429-2012, 2012.

Wu, S., Mickley, L. J., Jacob, D. J., Logan, J. A., Yantosca, R. M., and Rind, D.: Why are there large differences between models in global budgets of tropospheric ozone?, J. Geophys. Res.-Atmos., 112, D05302, doi:10.1029/2006jd007801, 2007.

Yang, F., Tan, J., Zhao, Q., Du, Z., He, K., Ma, Y., Duan, F., Chen, G., and Zhao, Q.: Characteristics of $PM_{2.5}$ speciation in representative megacities and across China, Atmos. Chem. Phys., 11, 5207–5219, doi:10.5194/acp-11-5207-2011, 2011.

Zhang, L., Jacob, D. J., Boersma, K. F., Jaffe, D. A., Olson, J. R., Bowman, K. W., Worden, J. R., Thompson, A. M., Avery, M. A., Cohen, R. C., Dibb, J. E., Flock, F. M., Fuelberg, H. E., Huey, L. G., McMillan, W. W., Singh, H. B., and Weinheimer, A. J.: Transpacific transport of ozone pollution and the effect of recent Asian emission increases on air quality in North America: an integrated analysis using satellite, aircraft, ozonesonde, and surface observations, Atmos. Chem. Phys., 8, 6117–6136, doi:10.5194/acp-8-6117-2008, 2008.

Zhang, Q., Streets, D. G., He, K., Wang, Y., Richter, A., Burrows, J. P., Uno, I., Jang, C. J., Chen, D., Yao, Z., and Lei, Y.: NO_x emission trends for China, 1995–2004: the view from the ground and the view from space, J. Geophys. Res., 112, D22306, doi:10.1029/2007JD008684, 2007.

Zhang, Q., Streets, D. G., and He, K. B.: Satellite observations of recent power plant construction in Inner Mongolia, China, Geophys. Res. Lett., 36, L15809, doi:10.1029/2009gl038984, 2009a.

Zhang, Q., Streets, D. G., Carmichael, G. R., He, K. B., Huo, H., Kannari, A., Klimont, Z., Park, I. S., Reddy, S., Fu, J. S., Chen, D., Duan, L., Lei, Y., Wang, L. T., and Yao, Z. L.: Asian emissions in 2006 for the NASA INTEX-B mission, Atmos. Chem. Phys., 9, 5131–5153, doi:10.5194/acp-9-5131-2009, 2009b.

Zhao, C. and Wang, Y. H.: Assimilated inversion of NO_x emissions over east Asia using OMI NO_2 column measurements, Geophys. Res. Lett., 36, L06805, doi:10.1029/2008gl037123, 2009.

Table 1. Sensitivity simulations by adjusting model meteorological or chemical parameters [1]

Case	Parameter	Adjustments	Notes & ref.
1	Base simulation	No changes in parameters	As in Lin (2012)
2	Air temperature in the lowest 10 layers (about 0–1.3 km)	Decreased by 2 °C in the daytime and increased by 1 °C at night	Based on ISH data
3[2]	Air temperature in the lowest 10 layers (about 0–1.3 km)	Decreased by 5 °C in the daytime and increased by 1 °C at night	Based on ISH data
4	Air temperature in the lowest four layers (about 0–0.5 km)	Decreased by 5 °C in the daytime and increased by 1 °C at night	Based on ISH data
5	Air temperature in the lowest 10 layers (about 0–1.3 km)	Increased by 5 °C at night	Based on ISH data
6	Tropospheric water vapor content	Scaled up by 130 %	Based on ISCCP data
7[2]	Tropospheric water vapor content	Scaled down by 130 %	Based on ISCCP data
8	Cloud optical depth	Assumed to be zero	Based on ISCCP data
9	Cloud optical depth	Decreased by 50 %	Based on ISCCP data
10	Cloud optical depth	Increased by 50 %	Based on ISCCP data
11[2]	Cloud optical depth	Increased by 100 %	Based on ISCCP data
12	Cloud optical depth	Evenly distributed in all tropospheric layers	Based on ISCCP data and Liu et al. (2009)
13	PBLH	Derived online	
14	PBLH	Decreased by 10 % in the daytime and tripled at night	Based on ISH temperature data and Liu et al. (2010)
15	PBLH	Tripled at night	Based on ISH temperature data and Liu et al. (2010)
16	PBLH	PBLH taken from GEOS-4	
17	PBLH	Scaled up by 130 %	To analyze potential causes of underestimated NO_2 columns
18	PBLH	Scaled up by 200 %	To analyze potential causes of underestimated NO_2 columns
19[2]	Rate constant for OH + NO_2 reaction	Scaled down by 130 %	Mollner et al. (2010); Sander et al. (2011)
20	Rate constant for OH + NO_2 reaction	Scaled up by 130 %	Mollner et al. (2010); Sander et al. (2011)
21	Yield of HNO_3 from NO + HO_2 reaction	Assumed to be 5 %	Butkovskaya et al. (2005, 2007, 2009); Sander et al. (2011)
22	Yield of HNO_3 from NO + HO_2 reaction	Assumed to be 1 %	Butkovskaya et al. (2005, 2007, 2009); Sander et al. (2011)
23[2]	OH regeneration from isoprene chemistry	Yield of 100 % from isoprene + OH reaction assumed	Butler et al. (2008); Lelieveld et al. (2008); Kubistin et al. (2010)
24	OH regeneration from isoprene chemistry	Isoprene + OH reaction turned off	Kubistin et al. (2010)
25[2]	Net yield of isoprene nitrates	Decreased from 10 % to 2.4 %	See review by Paulot et al. (2009). Transport of isoprene nitrates is neglected.
26	Equilibrium constant of PAN	Decreased by 20 %	Sander et al. (2011)
27[2]	Uptake rate of HO_2 on aerosols	Set at 0.2	Thornton et al. (2008); Jacob (2000); He et al. (2001); Yang et al. (2011)
28	Uptake rate of HO_2 on sulfate-nitrate-ammonium aerosols in the continental PBL	Set at 0.2	Thornton et al. (2008); Jacob (2000); He et al. (2001); Yang et al. (2011)
29[2]	Uptake rate of N_2O_5 on aerosols	Scaled down by a factor of 10	Bertram et al. (2009); Brown et al. (2009)
30[2]	Aerosol scattering and absorption	Turned off for all aerosols	Based on comparison with MODIS AOD
31	Aerosol scattering and absorption	Turned off for BC alone	Based on comparison with MODIS AOD
32	Emissions of CO and SO_2	Increased by 50 %	Following Lin et al. (2010b)
33	Emissions of propene	Increased by 50 %	To represent effects of aromatics based on INTEX-B inventory (Zhang et al., 2009)
34[2]	Emissions of propene	Increased by 300 %	To represent effects of aromatics based on top-down constraint (Liu et al., 2010, 2011)
35	Emissions of CO, SO_2 and VOC	Increased by 50 %	Following Lin et al. (2010b)

[1] Analyses are done in Sects. 4 and 5 also for other parameters without conducting additional sensitivity simulations.

[2] These cases are used for post-model modifications described in Table 2 and analyzed in Sects. 6 and 7.

Table 2. Parameters considered in post-model modification for NO_2 columns and surface ozone at the 284 meteorological stations in East China.

Parameter	Modifications	Case in Table 1 [1]	Impacts on NO_2 columns [2]	Impacts on surface ozone [2]	Notes & ref.
(a) Air temperature	Based on ISH values	3	Insignificant	Large in July and small in January	Modification is assumed for the lowest 10 layers
(b) Tropospheric water vapor content	Based on ISCCP values	7	Small in July and insignificant in January	Large	
(c) Cloud optical depth	Based on ISCCP values	11	Very large in July and insignificant in January	Large in July and very large in January	
(d) Rate constant of OH + NO_2 reaction	lowered by 15 %	19	Large in July and small in January	Small	Mollner et al. (2010); Sander et al. (2011)
(e) OH regeneration from isoprene chemistry	Yield of 100 % from isoprene + OH reaction assumed	23	Small in July and insignificant in January	Insignificant	Butler et al. (2008); Lelieveld et al. (2008); Kubistin et al. (2010)
(f) Net yield of isoprene nitrates	6 % instead of 10 %	25	insignificant	Insignificant	See review by Paulot et al. (2009)
(g) Uptake rate of HO_2 on aerosols	0.2 instead of the default setup; biases in model AOD with respect to MODIS accounted for	27	Very large	Very large	Thornton et al. (2008); Jacob, (2000); He et al. (2001); Yang et al. (2011)
(h) Uptake rate of N_2O_5 on aerosols	10 % of the default setup; biases in model AOD with respect to MODIS accounted for	29	Insignificant in July and large in January	Small in July and insignificant in January	Bertram et al. (2009); Brown et al. (2009)
(i) Aerosol scattering and absorption	Scaled based on MODIS AOD in comparison with model AOD	30	Insignificant	Insignificant in July and large in January	
(j) Emissions of propene	Increased by 300 %	34	Insignificant in July and large in January	Large in July and very large in January	To represent effects of aromatics based on top-down constraint (Liu et al., 2010, 2011)

[1] Results from sensitivity simulations described in Table 1 are used as the basis of respective post-model modifications here, i.e., they provide $\partial \ln \Omega / \partial P_i$ in Eq. (1) for individual parameters.

[2] Impacts with the slopes in Figs. 13–16 deviating from unity by more than 10 %, 5–10 %, 2–5 %, and within 2 % are indicated here as very large, large, small, and insignificant, respectively. For ozone, impacts are indicated also as large (very large) if the R^2 in Figs. 15, 16 is reduced to about 0.90–0.95 (lower than 0.90). Note that these indications are for the overall impact in East China; and impacts may be larger or smaller at individual stations.

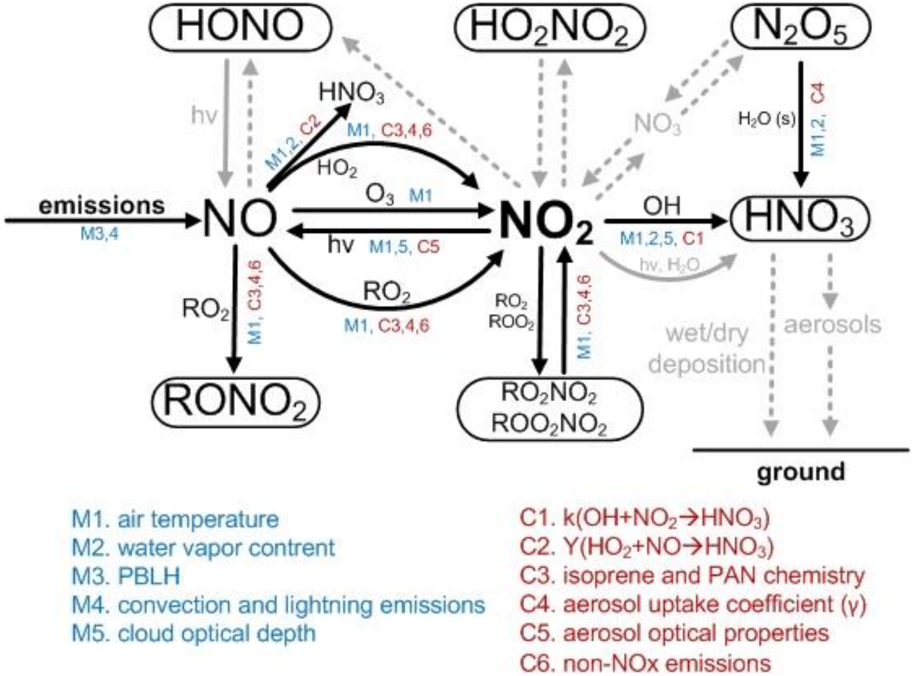

Fig. 1. Tropospheric chemistry involving NO_x and impacts of meteorological and chemical parameters evaluated in the present study. Processes shown in solid grey arrows are discussed without sensitivity simulations. Processes shown in dashed grey arrows are not discussed explicitly. Note that PBL mixing and convection affect vertical distributions of NO_x and related species. Heterogeneous uptake on aerosols depends on the amount of aerosol surfaces as well. Evaluation on the $RONO_2$ pathway is focused mainly on isoprene nitrates. Clouds and water vapor have indirect influences on radicals through effects on solar radiation.

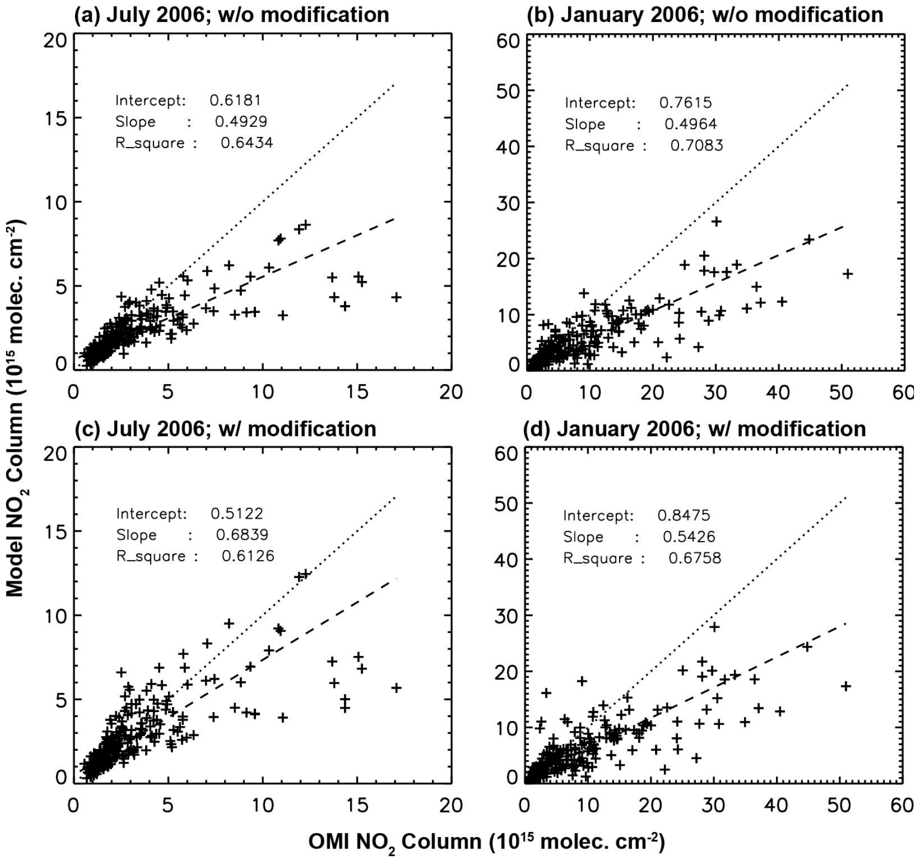

Fig. 2. Scatter plot for NO_2 columns at the 284 meteorological stations in East China retrieved from OMI and simulated by GEOS-Chem with and without post-model modifications discussed in Sect. 6. Also presented is the statistics from the RMA regression.

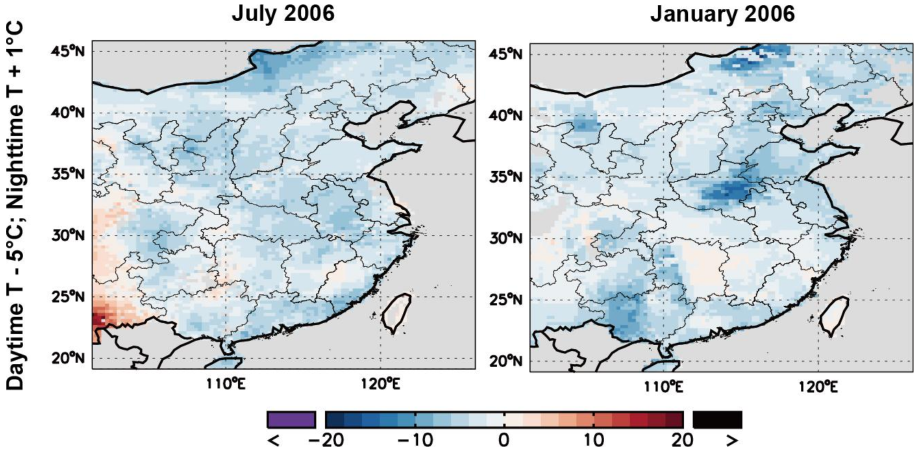

Fig. 3. Spatial distribution of percentage differences between modeled NO_2 columns with and without adjustments in air temperature: the daytime temperature is decreased by 5 °C with an increase of 1 °C at night for the lowest 10 model layers. See Fig. S9 for more results of sensitivity tests on temperature.

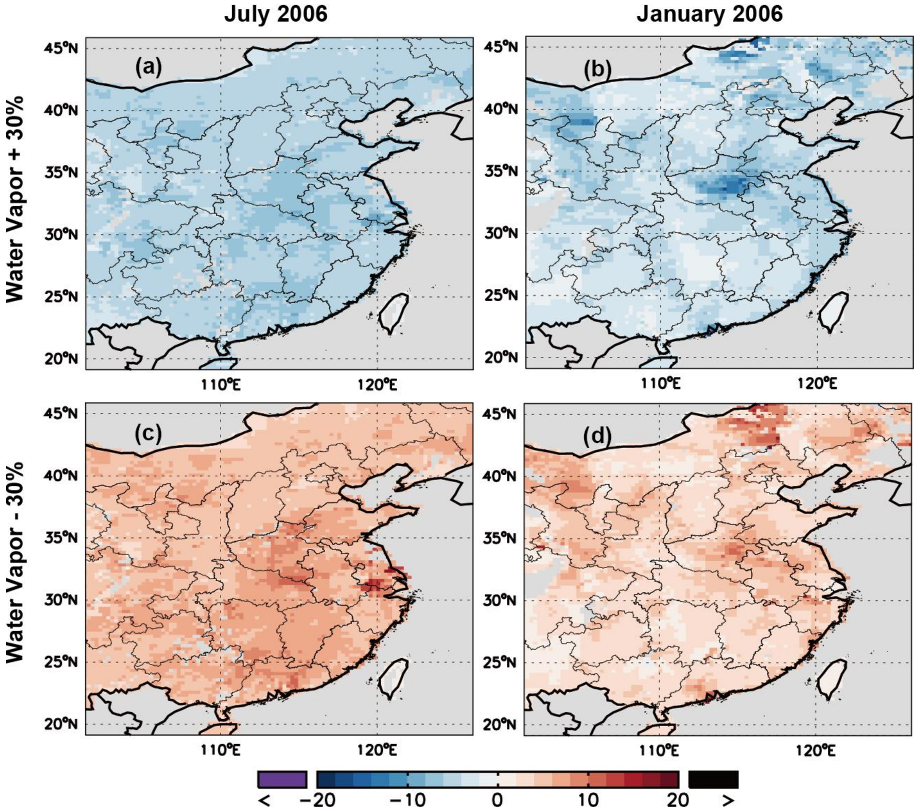

Fig. 4. Spatial distribution of percentage differences between modeled NO_2 columns with and without adjustments in tropospheric water vapor content. **(a, b)** The water vapor content is scaled up by 130 % in **(a, b)** and scaled down by 130 % in **(c, d)**.

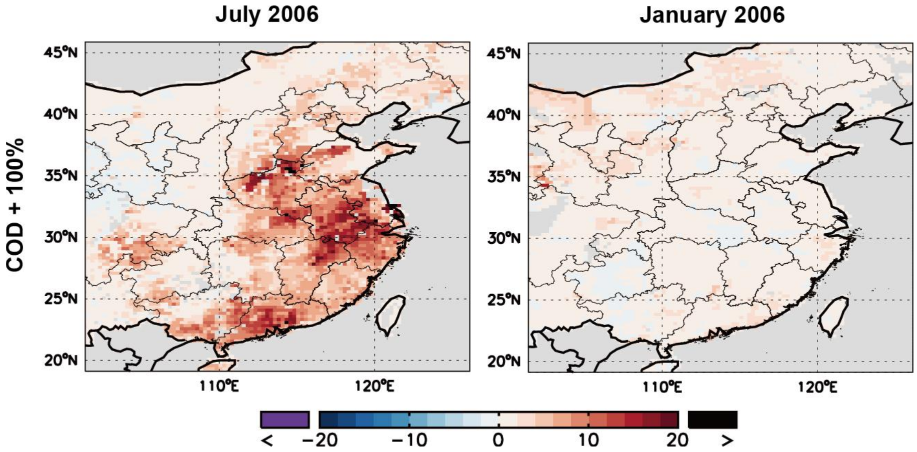

Fig. 5. Spatial distribution of percentage differences between modeled NO_2 columns with and without doubling the COD. See Fig. S10 for more results of sensitivity tests on COD.

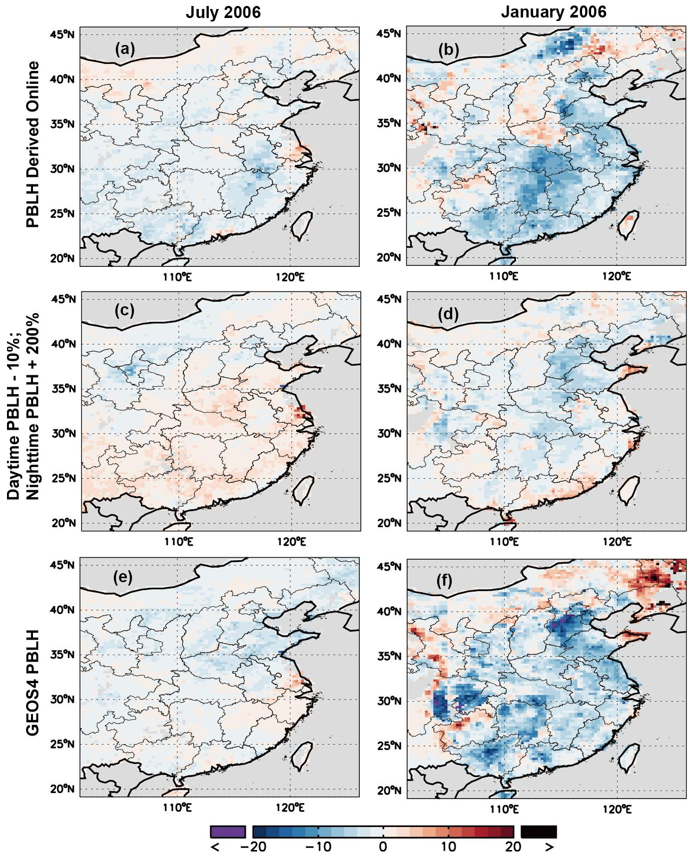

Fig. 6. Spatial distribution of percentage differences between modeled NO_2 columns with and without adjustments in PBLH. **(a, b)** The PBLH is calculated online by GEOS-Chem instead of being taken directly from GEOS-5. **(c, d)** The PBLH is decreased by 10 % in the daytime and tripled at night. **(e, f)** The PBLH is adjusted based on values from the GEOS-4 meteorological fields.

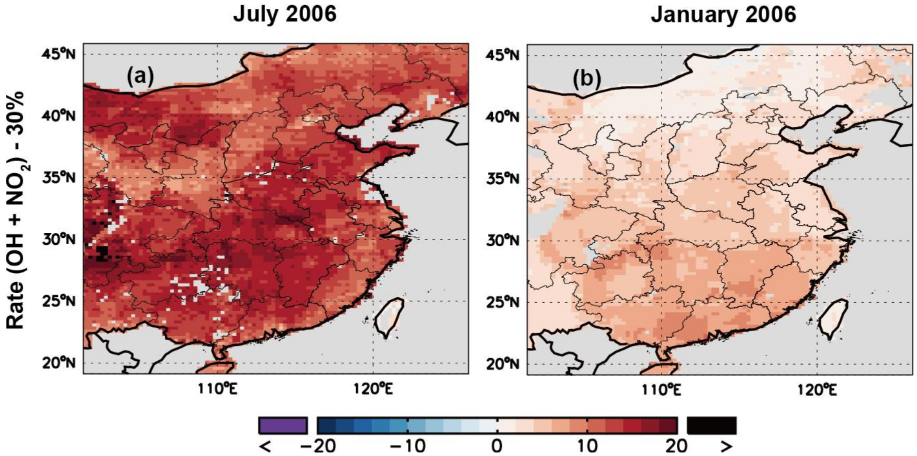

Fig. 7. Spatial distribution of percentage differences between modeled NO_2 columns with and without scaling down the rate constant of OH + NO_2 reaction by a factor of 130 %.

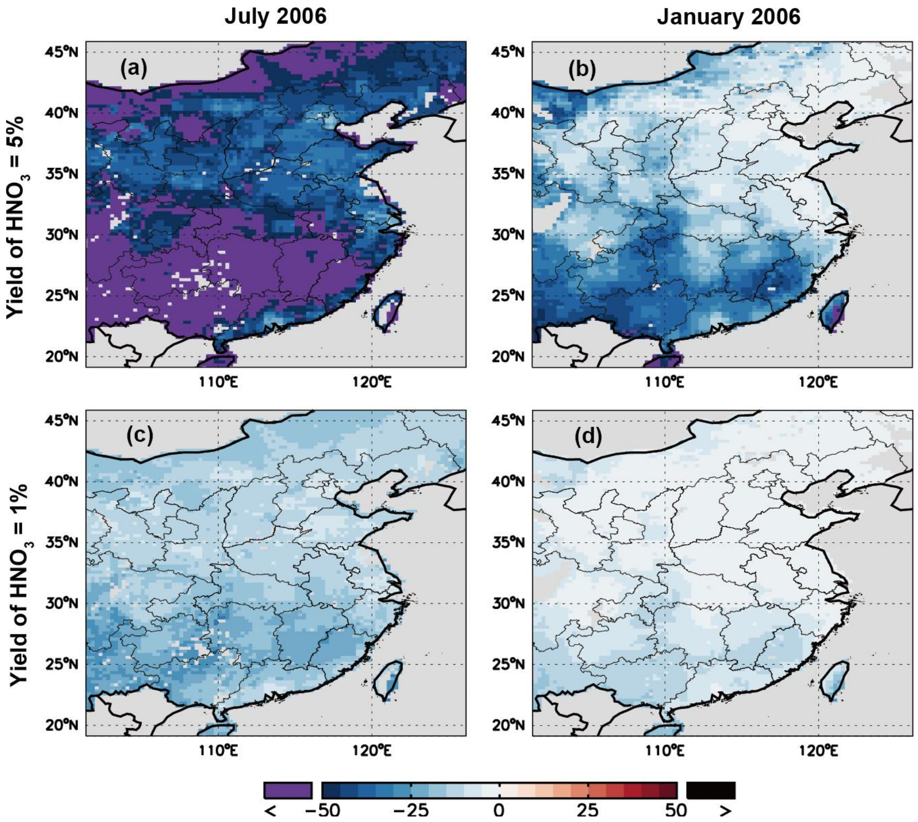

Fig. 8. Spatial distribution of percentage differences between modeled NO_2 columns with and without assuming a yield of HNO_3 at 5 % **(a, b)** or 1 % **(c, d)** from the $HO_2 + NO$ reaction.

Title Page
Abstract | Introduction
Conclusions | References
Tables | Figures
◀| |▶
◀ ▶
Back | Close
Full Screen / Esc
Printer-friendly Version
Interactive Discussion

Title Page
Abstract Introduction
Conclusions References
Tables Figures
◂◂ ▸▸
◂ ▸
Back Close
Full Screen / Esc
Printer-friendly Version
Interactive Discussion

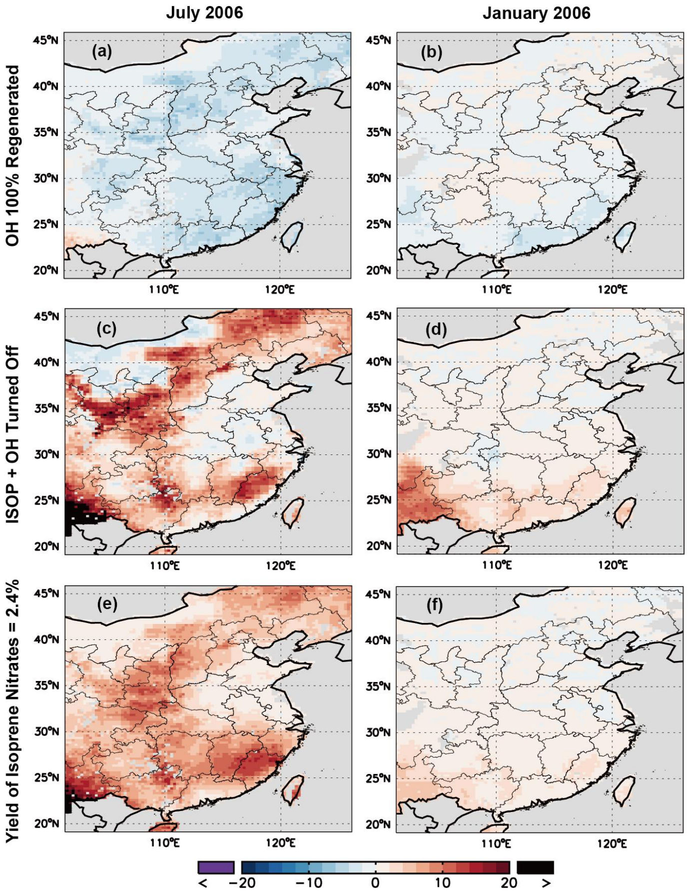

Fig. 9. Spatial distribution of percentage differences between modeled NO_2 columns with and without adjustments in the organic chemistry. **(a, b)** The OH is assumed to be 100 % regenerated from the reaction of isoprene + OH. **(c, d)** The isoprene + OH reaction is turned off. **(e, f)** The net yield of isoprene nitrates is assumed to be 2.4 % instead of the default 10 %.

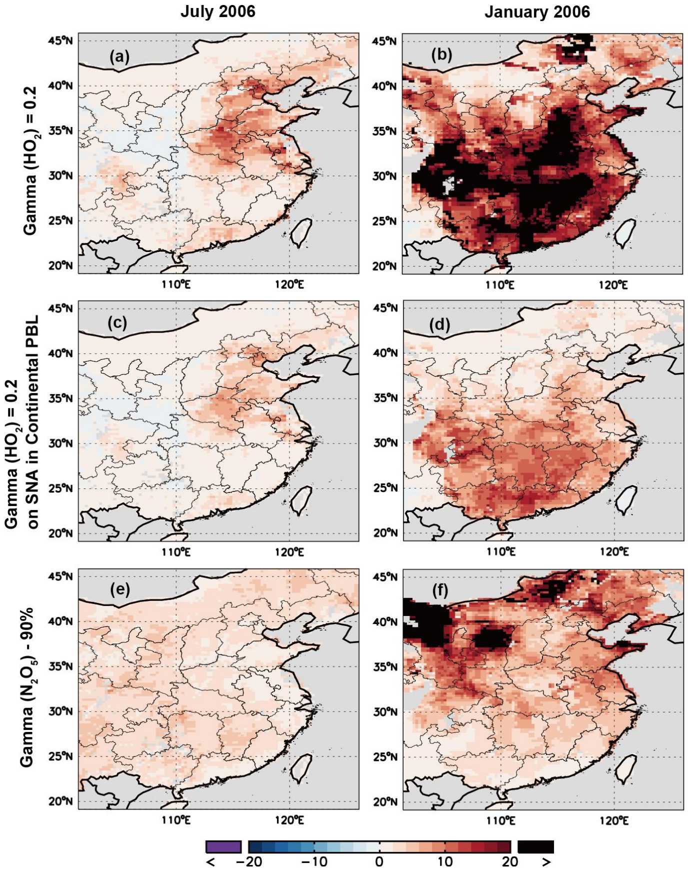

Fig. 10. Spatial distribution of percentage differences between modeled NO_2 columns with and without adjustments in the heterogeneous chemistry. **(a, b)** The uptake rate of HO_2 on aerosols is assumed to be 0.2. **(c, d)** The uptake rate of HO_2 on sulfate-nitrate-ammonium aerosols is assumed to be 0.2 in the continental boundary layer. **(e, f)** The uptake rate of N_2O_5 on aerosols is scaled down by a factor of 10.

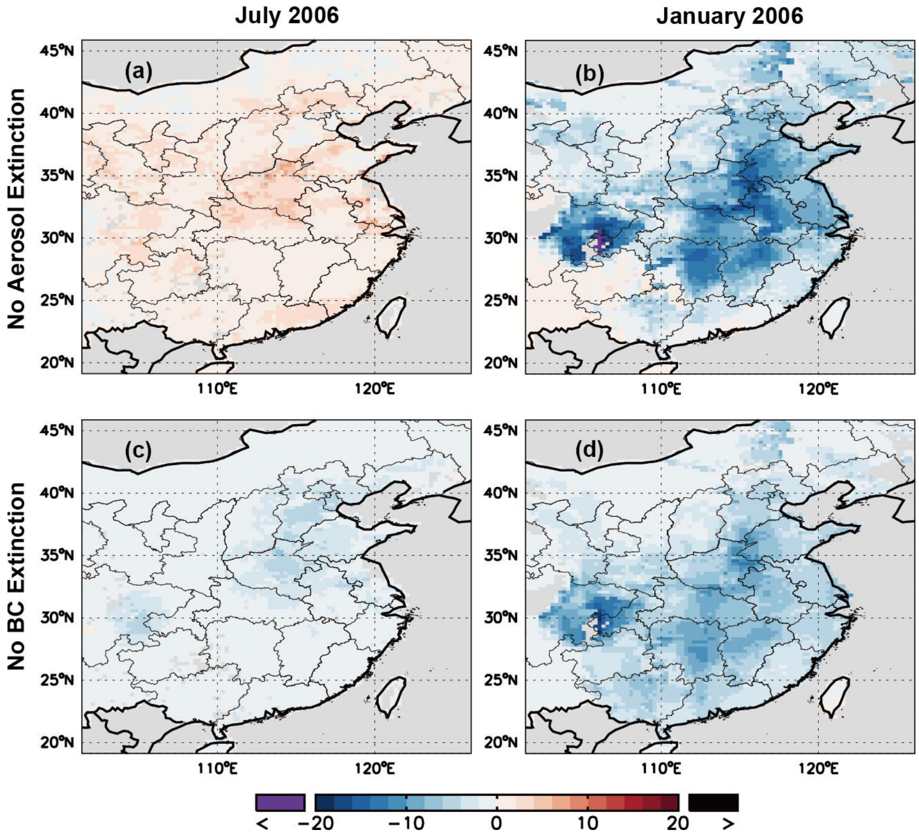

Fig. 11. Spatial distribution of percentage differences between modeled NO_2 columns with and without eliminating the scattering and absorption of radiation by all aerosols **(a, b)** or BC **(c, d)**.

ACPD
12, 14269–14327, 2012

Model uncertainties affecting NOx and ozone simulations

J.-T. Lin et al.

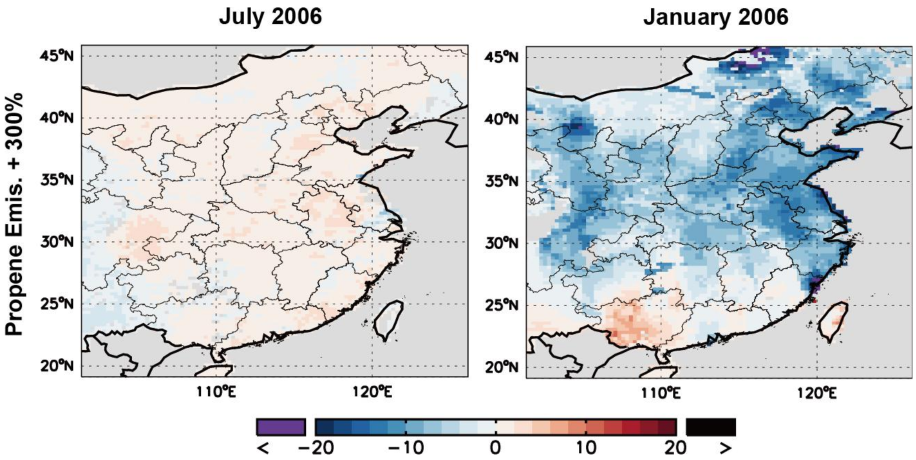

Fig. 12. Spatial distribution of percentage differences between modeled NO_2 columns with and without increasing emissions of propene by 300 %. See Fig. S16 for more results of sensitivity tests on non-NO_x emissions.

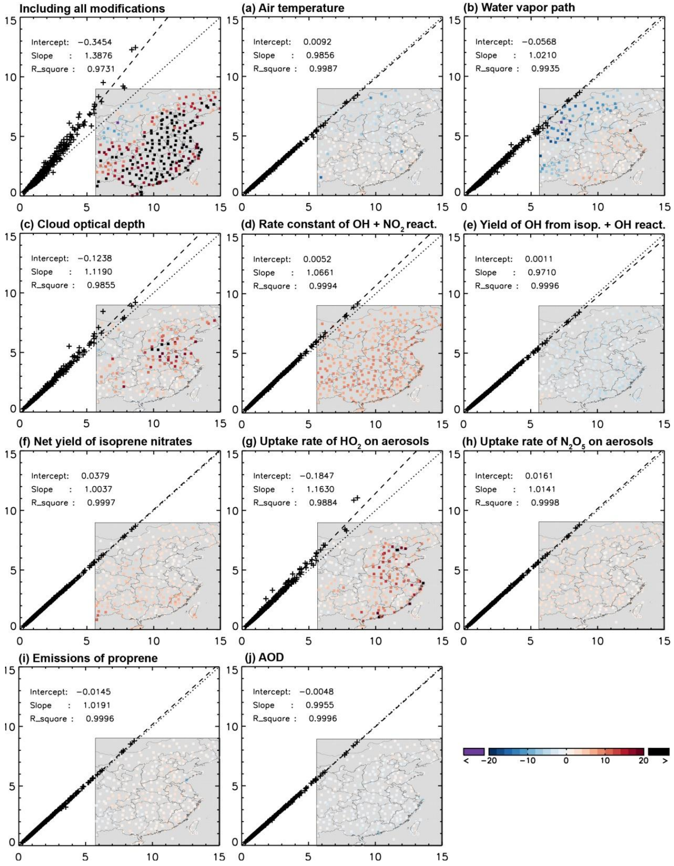

Fig. 13. Scatter plot for model NO_2 columns (10^{15} molecules cm^{-2}) in July 2006 without (x-axis) and with (y-axis) post-model modifications accounting for errors in meteorological and chemical parameters. Cases **(a–j)** are described in order in Table 2. Embedded in each panel are the respective statistics from the RMA regression and the spatial distribution of their percentage differences.

Title Page
Abstract
Introduction
Conclusions
References
Tables
Figures
◀I
▶I
◀
▶
Back
Close
Full Screen / Esc
Printer-friendly Version
Interactive Discussion

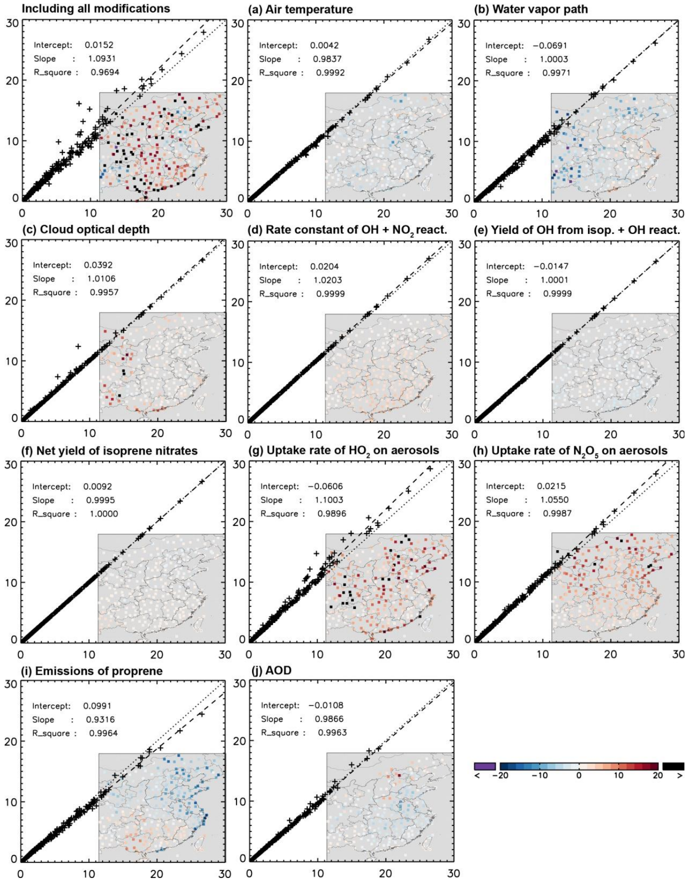

Fig. 14. Similar to Fig. 13 but for January 2006.

Discussion Paper | Discussion Paper | Discussion Paper | Discussion Paper |

ACPD

12, 14269–14327, 2012

Model uncertainties affecting NOx and ozone simulations

J.-T. Lin et al.

Title Page
Abstract Introduction
Conclusions References
Tables Figures
◀I ▶I
◀ ▶
Back Close
Full Screen / Esc

Printer-friendly Version

Interactive Discussion

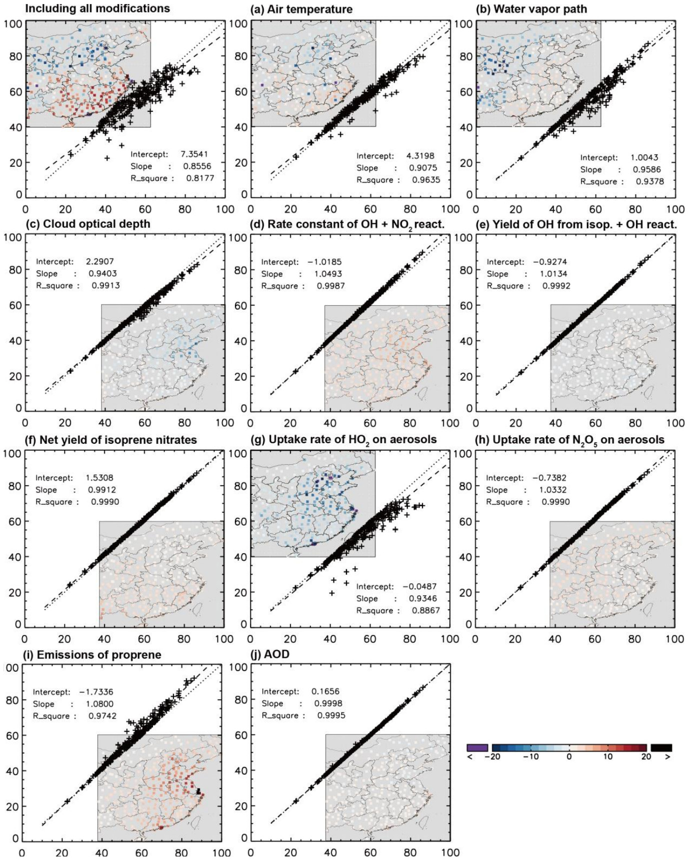

Fig. 15. Similar to Fig. 13 but for surface ozone (ppb) in July 2006.

Title Page
Abstract Introduction
Conclusions References
Tables Figures
◀ ▶
Back Close
Full Screen / Esc
Printer-friendly Version
Interactive Discussion

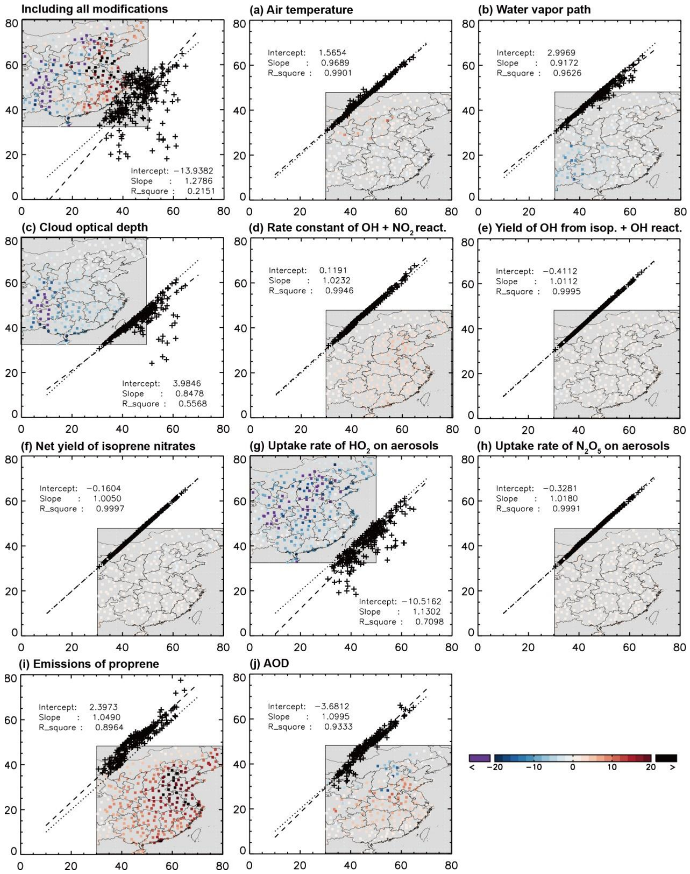

Fig. 16. Similar to Fig. 13 but for surface ozone (ppb) in January 2006.